Southern Blot Analysis

DNA was extracted from cardiac tissues, and a Southern blot analysis was performed to measure the mtDNA copy number as described earlier.[9] Primers for the mtDNA probe corresponded to nucleotides 2424 to 3605 of the mouse mitochondrial genome, and those for the nuclear-encoded mouse 18S rRNA probe corresponded to nucleotides 435 to 1951 of the human 18S rRNA genome. The mtDNA levels were normalized to the abundance of the 18S rRNA gene run on the same gel.

RNA Isolation and Northern Blot Analysis

Total RNA was isolated from frozen LV by the guanidinium method, and a Northern hybridization analysis was performed according to methods described previously.[9] Probes for mtRNA analysis were prepared by amplification of nucleotides 1209 to 2606 (probe 1), nucleotides 3351 to 7570 (probe 2), nucleotides 8861 to 14549 (probe 3), and nucleotides 14729 to 15837 (probe 4) of mtDNA from mouse genomic DNA.

Mitochondrial Enzyme Activity

The specific activity of complex I, complex II, complex III, and complex IV was measured in the myocardial tissues according to methods described previously.[9] The specific enzymatic activity of rotenone-sensitive NADH-ubiquinone oxidoreductase (complex I) was measured by a reduction of the ubiquinone analogue decylubiquinone. For the activity of succinate-ubiquinone oxidoreductase (complex II), the reduction of 2,6-dichlorophenolindophenol, when coupled to complex II–catalyzed reduction of decylubiquinone, was measured. For the specific activity of ubiquinol/cytochrome *c* oxidoreductase (complex III), the reduction of cytochrome *c* catalyzed by complex III in the presence of reduced decylubiquinone was monitored. The specific activity of cytochrome *c* oxidase (complex IV) was measured by following the oxidation of reduced cytochrome *c*, which had been prepared in the presence of dithionite. All enzymatic activities were expressed as nanomoles per minute per milligram protein.

Echocardiographic and Hemodynamic Measurements

After 4 weeks of surgery, echocardiographic studies were performed under light anesthesia with tribromoethanol/amylene hydrate (Avertin; 2.5% wt/vol, 8 μL/g IP) and spontaneous respiration. A 2D parasternal short-axis view of the LV was obtained at the level of the papillary muscles. In general, the best views were obtained with the transducer lightly applied to the mid upper left anterior chest wall. The transducer was then gently moved cephalad or caudad and angulated until desirable images were obtained. After it was ensured that the imaging was on axis (based on roundness of the LV cavity), 2D targeted M-mode tracings were recorded at a paper speed of 50 mm/s. Our previous study has shown that the intraobserver and interobserver variabilities of our echocardiographic measurements for LV dimensions were small, and measurements made in the same animals on separate days were highly reproducible.[17] Then, under the same anesthesia with Avertin, a 1.4F micromanometer-tipped catheter (Millar Instruments) was inserted into the right carotid artery and then advanced into the LV to measure pressures.[17]

Infarct Size

To measure the infarct size after 28 days of MI, the heart was excised, and the LVs were cut from apex to base into 3 transverse sections. Five-micrometer sections were cut and stained with Masson's trichrome. Infarct length was measured along the endocardial and epicardial surfaces from each of the cardiac sections, and the values from all specimens were summed. Infarct size (in percentage) was calculated as total infarct circumference divided by total cardiac circumference.[17]

In addition, to measure infarct size after 24 hours when most animals are still alive, a separate group of animals including WT-MI (n=6) and Tg-MI (n=6) was created. After 24 hours of coronary artery ligation, Evans blue dye (1%) was perfused into the aorta and coronary arteries, and tissue sections were weighed and then incubated with a 1.5% triphenyltetrazolium chloride solution. The infarct area (pale), the area at risk (not blue), and the total LV area from each section were measured.[18] In our preliminary study, we confirmed excellent reliability of infarct size measurements, in which a morphometric methodology similar to that used in this study was used. The intraobserver and interobserver variabilities between 2 measurements divided by these means, expressed as a percentage, were <5%.

Histopathology

After in vivo hemodynamic studies, the heart was excised and dissected into the right and left ventricles, including the septum. Five-micrometer sections were cut and stained with Masson's trichrome. Myocyte cross-sectional area and collagen volume fraction were determined by the quantitative morphometry of LV tissue sections.[17]

For assessment of mitochondrial ultrastructure by electron microscopy, LV tissues were fixed in a mixture of 1% glutaraldehyde and 4% paraformaldehyde in 0.1 mol/L phosphate buffer at pH 7.4 for 2 hours at room temperature. After they were washed in 0.1 mol/L phosphate buffer containing 0.25 mol/L sucrose, they were postfixed with 1% osmium tetroxide for 1 hour at room temperature. The tissues were then block-stained with 1% uranyl acetate in 50% methanol for 2 hours, dehydrated in a graded series of ethanol, and embedded in Epon. Ultrathin sections were double stained with uranyl acetate and lead citrate and then were observed under an electron microscope (Hitachi H7000). For quantitative morphometric analysis, the number and size of the mitochondria were examined according to methods described previously.[9] The number of mitochondria and the cross-sectional area (size) of each mitochondrion were measured within a sampling region of 100 square sarcomeres (sm^2). Eighteen regions were selected at random for each specimen, and for all regions the averages of mitochondrial number and cross-sectional area were calculated.

Apoptosis

To detect apoptosis, LV tissue sections were stained with terminal deoxynucleotidyl transferase–mediated dUTP nick end-labeling (TUNEL) staining. The number of TUNEL-positive cardiac myocyte nuclei was counted, and the data were normalized per 10^5 total nuclei identified by hematoxylin-positive staining in the same sections. We further examined whether apoptosis is present by the more sensitive ligation-mediated PCR fragmentation assays (Maxim Biotech Inc).[18]

Statistical Analysis

Data are expressed as mean±SEM. Survival analysis was performed by the Kaplan-Meier method, and between-group difference in survival was tested by the log-rank test. Between-group comparison of means was performed by 1-way ANOVA, followed by *t* tests. The Bonferroni correction was done for multiple comparisons of means. $P<0.05$ was considered statistically significant.

Results

Characterization of Human TFAM Tg Mice

Human *TFAM* cDNA was used to generate Tg mice (Figure 1A). Four lines of Tg mice were confirmed by PCR. These lines were viable and fertile, and there were no detectable differences in cardiac size and structure between Tg and WT mice either macroscopically or microscopically.

We analyzed TFAM protein levels in various tissues by Western blot analysis using anti-human TFAM antibody. We found a robust expression of human TFAM protein in the heart and skeletal muscle, but it was barely detected in the lung, liver, and kidney (Figure 1B). Among 4 established lines of Tg mice, 1 line that expressed the highest level of the human TFAM protein in the heart was used for further

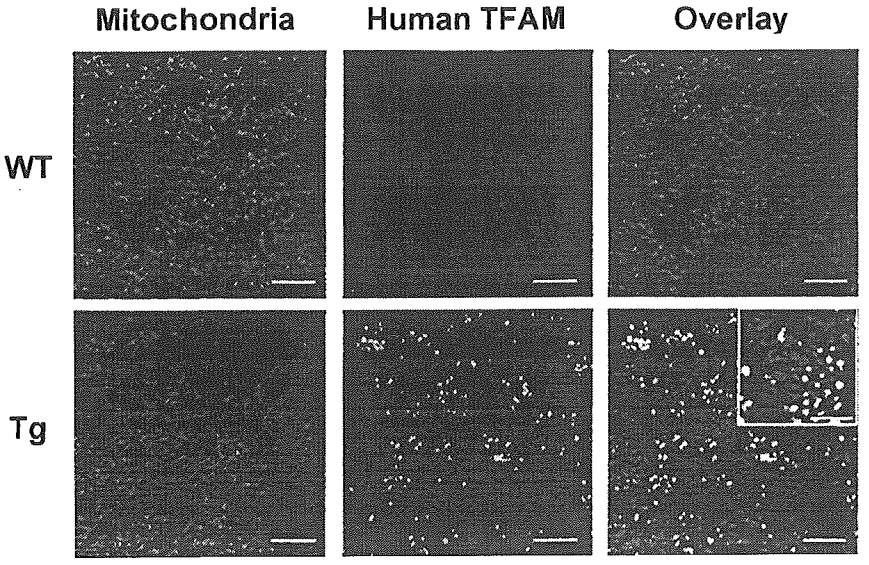

Figure 2. Myocardial tissue sections from WT (top) and Tg (bottom) mice were double-stained with MitoTracker dye (red) and a human TFAM specific antibody (green). Immunoreactivity for human TFAM was observed in the cytoplasm of cardiac myocytes. Merged images show that TFAM was colocalized with the mitochondria (yellow). Bar=20 μm. Inset shows merged images with higher magnification; bar=10 μm.

experiments. The endogenous expression level of the mouse Tfam protein was not modified or downregulated by the overexpression of human *TFAM* gene (Figure 1C). Immunohistochemical studies showed homogeneous human TFAM distribution in cardiac myocytes and colocalized with the mouse mitochondria (Figure 2). Human TFAM staining showed a relatively spotty staining pattern. With higher magnification, its expression appeared not to be restricted to a specific site of mitochondria (Figure 2, inset). These results suggest that the human TFAM exerts an expression pattern similar to that observed for the endogenous mouse Tfam and may function in the mouse heart.

MtDNA Copy Number and Mitochondrial Enzymes

We created MI in male Tg mice (Tg-MI) and nontransgenic wild-type littermates (WT-MI). Sham operation without coronary artery ligation was also performed in WT (WT-sham) and Tg (Tg-sham) mice. After 4 weeks of surgery, we measured mtDNA copy number, expressed as the ratio of mtDNA to nuclear DNA (18S rRNA), in the myocardial tissue by a Southern blot analysis. In parallel to an increase in TFAM protein, mtDNA copy number increased in the heart from Tg animals compared with WT controls (Figure 3A). In WT-MI animals, mtDNA copy number in the noninfarcted LV showed a 41% decrease ($P<0.01$) compared with sham mice, which was significantly prevented and preserved at a normal level in Tg-MI mice (Figure 3A).

To determine the effects of mtDNA copy number alterations on mtRNA, mtRNA transcript levels were measured by Northern blot analysis. As previously reported,[9] mtRNA transcript levels, including ND1+ND2, ND4, ND4L, ND5, cytochrome *b*, COI, COII, and COIII transcripts as well as 16S rRNA, were lower in WT-MI than those in WT-sham. However, overexpression of human *TFAM* did not increase, and even decreased, these mRNA levels in Tg-sham as well as in Tg-MI (online-only Data Supplement I). These results indicate that the regulation of mtRNA transcripts is dissociated from that of mtDNA copy number.

We next measured the respiratory chain enzyme activities. Despite the significant increase in mtDNA copy number in the heart from Tg, complex I, complex II, complex III, and complex IV demonstrated no significant changes in the enzymatic activity in comparison with WT controls (Figure 3B). Consistent with mtDNA copy number, the enzymatic activities of complex I, complex III, and complex IV were significantly lower in the noninfarcted LV from WT-MI than those from WT-sham. Most importantly, there was no such decrease observed in Tg-MI (Figure 3B). The enzymatic activity of complex II, exclusively encoded by nuclear DNA, was not altered in either group. These results indicate that mtDNA and mitochondrial enzymatic activities are downregulated in the hearts after MI, and human *TFAM* gene overexpression efficiently counteracts these mitochondrial deficiencies.

The overall number of mitochondria and the overall average size of the mitochondria demonstrated no significant changes in Tg-sham in comparison with WT controls. In contrast, the mitochondrial number was significantly increased and their size was decreased in WT-MI, both of which were attenuated in Tg-MI (online-only Data Supplement II).

Survival

The survival analysis was performed in 4 groups of mice during the study period of 4 weeks; WT-sham (n=20), WT-MI (n=21), Tg-sham (n=29), and Tg-MI (n=29). There were no deaths in sham-operated groups. The survival rate was significantly higher in Tg-MI compared with WT-MI (100% versus 66%; $P<0.01$; Figure 4A).

Infarct Size

We determined the infarct size by morphometric analysis in the surviving mice 28 days after MI, and it was comparable between WT-MI and Tg-MI (Figure 4B). To further confirm that overexpression of *TFAM* gene did not alter the infarct size, both area at risk and infarct area were measured in a separate group of mice 24 hours after coronary artery ligation.

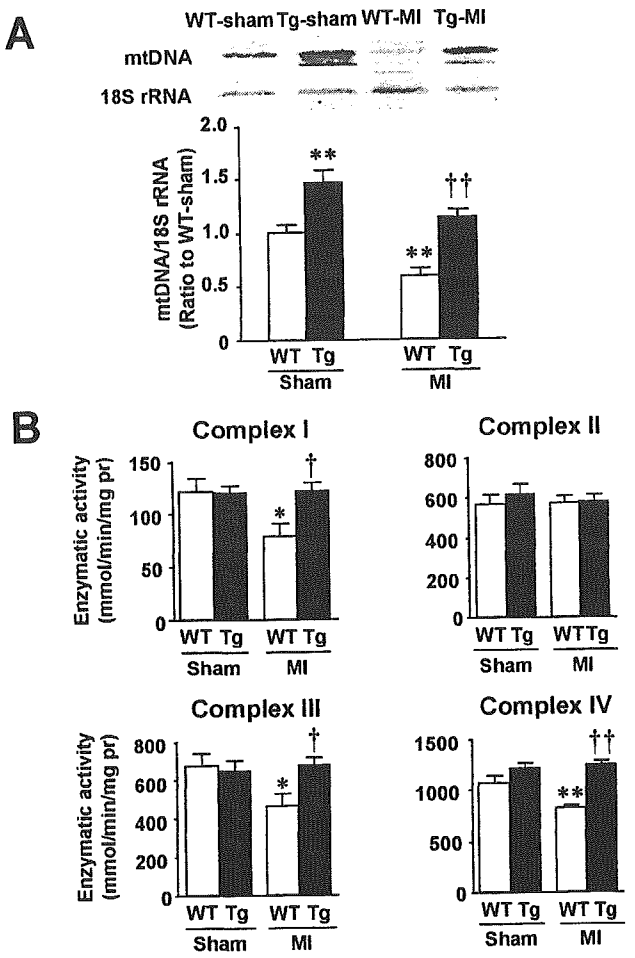

Figure 3. mtDNA and mitochondrial function. A, top, Southern blot analysis of mtDNA copy number in total DNA extracts from the heart from WT-sham, Tg-sham, WT-MI, and Tg-MI mice. Top bands show signals from the mtDNA fragment, and bottom bands show signals from the nuclear DNA fragment containing the 18S rRNA gene. A, bottom, Summary data for a Southern blot analysis of mtDNA copy number in 4 groups of animals (n=8 for each). Data were obtained by a densitometric quantification of the Southern blots such as those shown in A. B, Enzymatic activity of respiratory chain complex I, complex II, complex III, and complex IV in isolated mitochondria from 4 groups of animals (n=6 for each). Each assay was done in triplicate. Values are mean±SEM. *P<0.05, **P<0.01 for difference from WT-sham values. †P<0.05, ††P<0.01 for difference from WT-MI values. pr indicates protein.

The infarct size (infarct/risk area) was also comparable between WT-MI and Tg-MI mice (84.5±0.4% for n=6 versus 83.2±1.1% for n=6; P=NS; Figure 4C).

Cardiac Function and Structure

The echocardiographic studies of surviving mice at 4 weeks showed that cardiac diameters were significantly increased in WT-MI over the values in WT-sham or Tg-sham. Tg-MI showed less cavity dilatation and improved contractile function compared with WT-MI (Figure 5).

There was no significant difference in heart rate and aortic blood pressure among 4 groups of mice (Table). LV end-diastolic pressure increased in WT-MI and was significantly attenuated in Tg-MI. Coinciding with increased LV end-diastolic pressure, lung weight/body weight increased in WT-MI

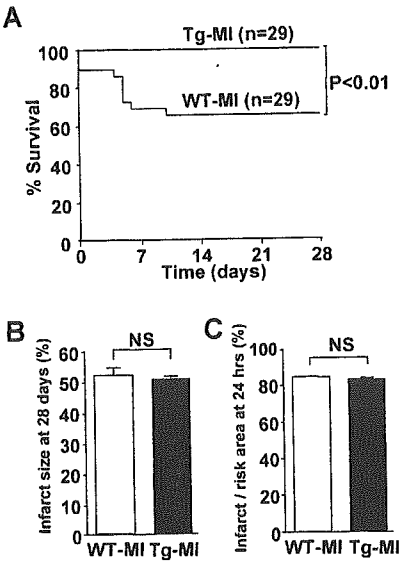

Figure 4. Survival and infarct size. A, Kaplan-Meier survival analysis. Percentages of surviving WT-MI (n=29) and Tg-MI (n=29) mice were plotted. Between-group difference was tested by the log-rank test. B, Infarct size values from WT-MI (n=6) and Tg-MI (n=6) mice in surviving mice 28 days after MI. C, Infarct size (infarct/risk area) values from WT-MI (n=6) and Tg-MI (n=6) mice 24 hours after MI. Values are mean±SEM.

and was also attenuated in Tg-MI (Table). The prevalence of pleural effusion, a clinical sign of heart failure, was significantly lower in Tg-MI than that in WT-MI (Table).

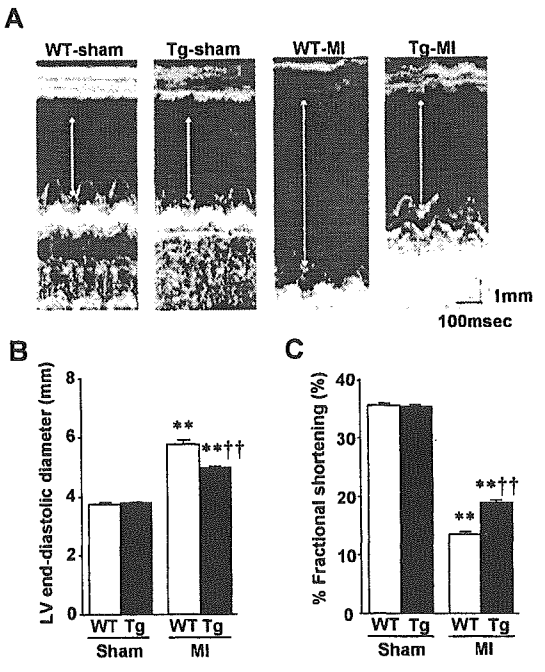

Figure 5. A, Representative M-mode echocardiograms obtained from WT-sham, Tg-sham, WT-MI, and Tg-MI mice. Arrows indicate LV end-diastolic diameter. B, C, Summary data for echocardiographic measurements in 4 groups of animals (n=6 for each). LV end-diastolic diameter (B) and percent fractional shortening (C) are shown. Values are mean±SEM. **P<0.01 for difference from WT-sham values; ††P<0.01 for difference from WT-MI values.

Characteristics of Animal Models

	WT-Sham (n=20)	Tg-Sham (n=21)	WT-MI (n=19)	Tg-MI (n=29)
Hemodynamic data				
Heart rate, bpm	469±6	471±4	479±11	477±4
Mean aortic pressure, mm Hg	77±4	76±2	73±1	74±1
LV EDP, mm Hg	0.7±0.5	0.7±0.4	13.1±2.0**	4.3±0.8*‡
Organ weight data				
Body weight, g	27.3±0.4	26.7±0.4	26.2±0.5	26.0±0.2
LV weight/body weight, mg/g	3.14±0.07	3.23±0.05	3.88±0.24**	3.69±0.09**
RV weight/body weight, mg/g	0.95±0.05	0.98±0.04	1.39±0.12**	1.12±0.05†
Lung weight/body weight, mg/g	5.3±0.1	5.3±0.1	8.3±0.6**	6.4±0.3‡
Pleural effusion, %	0	0	63**	31**†

Values are mean±SEM. EDP indicates end-diastolic pressure; RV, right ventricular.
**$P<0.01$ vs WT-sham; †$P<0.05$, ‡$P<0.01$ vs WT-MI.

Cross-sectional area of cardiac myocytes, an index of cellular hypertrophy, increased in the noninfarcted LV from WT-MI and was significantly attenuated in Tg-MI (Figure 6A). Collagen volume fraction, an index of myocardial interstitial fibrosis, also increased in the noninfarcted LV from WT-MI and was significantly smaller in Tg-MI (Figure 6B). These results indicate that TFAM efficiently counteracts structural and functional deterioration in post-MI hearts.

Apoptosis

To detect apoptosis, myocardial tissue sections were stained with TUNEL staining. TUNEL-positive nuclei were rarely seen in control mice, whereas their number increased in the noninfarcted LV from WT-MI and was significantly decreased in Tg-MI (Figure 7A). In addition, DNA ladder appeared faint in the noninfarcted LV from Tg-MI compared with that from WT-MI, suggesting the attenuation of apoptosis by *TFAM* overexpression (Figure 7B).

Discussion

The present study provides the first direct evidence that the overexpression of *TFAM* can prevent the decline in mtDNA as well as mitochondrial respiratory defects in post-MI hearts. TFAM significantly attenuated cardiac chamber dilatation and dysfunction as well as histopathological changes such as myocyte hypertrophy, interstitial fibrosis, and apoptosis. The apparent beneficial effects of *TFAM* overexpression were not due to its MI size–sparing effect, but they occurred secondary to more adaptive remodeling. All of these beneficial effects could contribute to the improved survival in Tg mice after MI.

Previous studies have suggested an intimate link between mtDNA damage, increased lipid peroxidation, and a decrease in mitochondrial electron transport complex enzyme activities.[4] A growing body of evidence suggests that mtDNA deficiencies and mitochondrial dysfunction play a major role in the development and progression of cardiac failure. A recent study from our laboratory demonstrated a decline in TFAM and mtDNA copy number in a murine heart failure model after MI.[9] These studies imply a relationship between TFAM, mtDNA copy

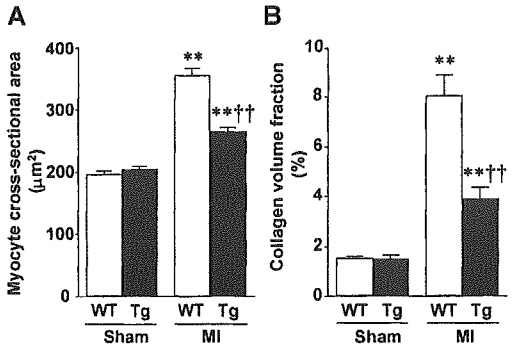

Figure 6. Summary data for histopathological analysis of LV tissue sections in 4 groups of animals (n=6 for each). Myocyte cross-sectional area (A) and collagen volume fraction (B) are shown. Values are mean±SEM. **$P<0.01$ for difference from WT-sham values; ††$P<0.01$ for difference from WT-MI values.

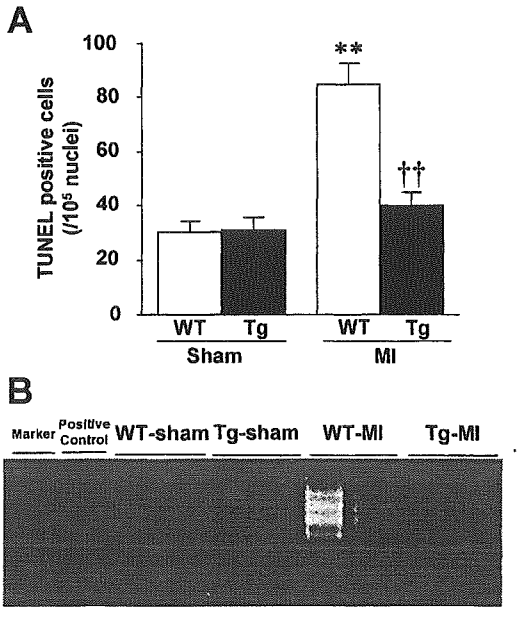

Figure 7. A, Number of TUNEL-positive myocytes in noninfarcted area of LV from 4 groups of animals (n=8 each). Values are mean±SEM. **$P<0.01$ for difference from WT-sham values. ††$P<0.01$ for difference from WT-MI values. B, DNA ladder indicative of apoptosis in genomic DNA from LV.

number, and mitochondrial function because the magnitude of the mtDNA defects is parallel to quantitative deficiencies in electron transport function. We thus proposed a direct relationship between TFAM content and electron transport chain activity during the post-MI remodeling process, ignoring the possibility of direct ischemic damage to the electron transport chain complexes. The downregulation of *TFAM* gene expression and a concurrent decrease in mitochondrial genes have been also shown in heart failure induced by aortic banding.[15] In addition, mtDNA depletion has been reported in mitochondrial myopathy and respiratory defects.[19–21] On the basis of these studies, mtDNA defects are considered to be involved not only in the pathogenesis of the diseases caused by inherited defects of mtDNA but also in those secondary to ischemia or mechanical overload.

TFAM not only regulates mtDNA transcription and replication[22] but also maintains mtDNA copy number. In fact, *Tfam* knockout mice, which had a 50% reduction in their transcript and protein levels, exerted a 34% reduction in the mtDNA copy number, 22% reduction in the mitochondrial transcript levels, and partial reduction in the cytochrome *c* oxidase levels in the heart.[11] Moreover, cardiac-specific disruption in the *Tfam* gene in mice exhibited dilated cardiomyopathy in association with a reduced amount of mtDNA and mitochondrial transcripts.[13] The transfection of antisense plasmids in culture, designed to reduce the expression of *TFAM*, effectively decreased the levels of mitochondrially encoded transcripts.[23] On the contrary, the forced overexpression of *TFAM* could produce the opposite effect.[24] Consistent with the present results (Figure 3A, 3B), a recent study by Ekstrand et al[25] demonstrated that the overexpression of human *TFAM* in the mouse increased mtDNA copy number. These lines of evidence imply the primary importance of TFAM as a regulatory mechanism of mtDNA copy number. TFAM has been shown to directly interact with mtDNA to form nucleoids.[26,27] Therefore, increased TFAM may increase the steady-state levels of mtDNA by directly binding and stabilizing mtDNA in Tg-sham mice. Our study also showed that overexpression of human *TFAM* did not increase the respiratory chain complex enzyme activities in Tg-sham mice (Figure 3C), suggesting that the regulation of mtDNA copy number is dissociated from that of electron transport function.[25] Furthermore, our proposed association between TFAM, mtDNA copy number, and electron transport chain activity may be weakened by our data that *TFAM* overexpression did not affect mtRNA levels (online-only Data Supplement I). There may be complex regulatory mechanisms responsible for the association of TFAM, mtDNA, and mitochondrial function, and further studies are clearly needed to solve this issue.

The results obtained from human *TFAM* Tg-sham mice differ from those from the inducible, cardiac-specific overexpression of peroxisome proliferator-activated receptor γ coactivator-1α (PGC-1α) transgene in adult mice, which leads to a modest increase in mitochondrial number and development of reversible cardiomyopathy.[28] PGC-1α is the transcriptional coactivator and acts upstream of TFAM and also has the capacity to increase mtDNA levels as well as mitochondrial mass in cultured cells and in Tg mice.[29,30] The reason for the discrepant results between PGC-1 and TFAM transgene overexpression remains unsolved in this study, which, however, may be related to the complex regulatory mechanisms of mitochondrial biogenesis and function by PGC-1 and its downstream factors, including nuclear respiratory factors 1 and 2 and TFAM.[31,32] This may also be due to the difference in the timing of transgene overexpression. Moreover, even though the present study demonstrated the beneficial effects of *TFAM* overexpression on post-MI LV remodeling, it could not determine whether it must occur before the ischemic insult or only during the post-MI phase.

The present study clearly demonstrated that *TFAM* overexpression could ameliorate the decline in mtDNA copy number and preserve it at a normal level in hearts from Tg-MI mice (Figure 3A). *TFAM* overexpression might increase the steady-state levels of mtDNA by directly stabilizing mtDNA. Consistent with alterations in mtDNA, the decrease in oxidative capacities seen in MI was also prevented (Figure 3B). Moreover, our studies establish an important role of TFAM in myocardial protection against remodeling and failure (Figures 4A and 5). The beneficial effects of *TFAM* overexpression shown in the present study were not due to its MI size–sparing effect because infarct size was comparable between WT-MI and Tg-MI mice (Figure 4B, 4C). Furthermore, its effects were not due to the effects on hemodynamics because blood pressure and heart rate were not altered (Table).

Several factors may be attributable to the protective effects conferred by TFAM against myocardial remodeling and failure. First, *TFAM* overexpression prevented the decrease in mtDNA copy number (Figure 3A) and mitochondrial electron transport function (Figure 3B), which may contribute to the decrease in myocardial oxidative stress. The decreased oxidative stress could contribute to the amelioration of cardiac hypertrophy, apoptosis, and interstitial fibrosis.[18] Second, *TFAM* overexpression may induce mitochondrial biogenesis, which, however, is thought to be unlikely because the number and size of the mitochondria assessed by electron microscopy were not altered in Tg-sham mice (online-only Data Supplement II). Importantly, the beneficial effects of *TFAM* overexpression on LV remodeling and failure occurred with the attenuation of increased mitochondrial number seen in MI. Furthermore, an increase in mitochondrial number itself did not necessarily exert beneficial effects in MI.

Several pathogenic mtDNA base substitution mutations, such as missense mutations and mtDNA rearrangement mutations (deletions and insertions), have been identified in patients with mitochondrial diseases.[4] An accumulation of the deleted forms of mtDNA in the myocardium frequently results in either cardiac hypertrophy, conduction block, or heart failure.[33] Furthermore, there is now a consensus view that mutations in mtDNA and abnormalities in mitochondrial function are associated with common forms of cardiac diseases, such as ischemic heart disease[34] and dilated cardiomyopathy.[35] In these conditions, however, the strict causal relationship between abnormalities in mtDNA and cardiac dysfunction has yet to be fully elucidated.

The present study supports our earlier conclusions that the deficiencies of mtDNA contribute to cardiac failure.[9] Furthermore, it confirms that the defects in TFAM are critically involved in mitochondrial dysfunction as well as maladaptive cardiac remodeling and failure. More importantly, the increased

TFAM expression could ameliorate the pathophysiological processes seen in heart failure. MtDNA decline and mitochondrial defects are now well recognized in a variety of diseases such as neurodegenerative diseases, diabetes mellitus, cancer, and even aging. Therefore, with further knowledge on the mechanisms of TFAM for maintenance of mtDNA copy number and mitochondrial function, it may eventually be possible to develop novel strategies for the treatment of such diseases based on the manipulation of TFAM.

Acknowledgments

This study was supported in part by grants from the Ministry of Education, Science, and Culture (Nos. 09670724, 12670676, 14370230). A part of this study was conducted in Kyushu University Station for Collaborative Research I and II.

References

1. Attardi G, Schatz G. Biogenesis of mitochondria. *Annu Rev Cell Biol.* 1988;4:289–333.
2. Shadel GS, Clayton DA. Mitochondrial DNA maintenance in vertebrates. *Annu Rev Biochem.* 1997;66:409–435.
3. Clayton DA. Replication and transcription of vertebrate mitochondrial DNA. *Annu Rev Cell Biol.* 1991;7:453–478.
4. Wallace DC. Mitochondrial diseases in man and mouse. *Science.* 1999; 283:1482–1488.
5. Kajander OA, Karhunen PJ, Jacobs HT. The relationship between somatic mtDNA rearrangements, human heart disease and aging. *Hum Mol Genet.* 2002;11:317–324.
6. Naya FJ, Black BL, Wu H, Bassel-Duby R, Richardson JA, Hill JA, Olson EN. Mitochondrial deficiency and cardiac sudden death in mice lacking the MEF2A transcription factor. *Nat Med.* 2002;8:1303–1309.
7. Lebrecht D, Setzer B, Ketelsen UP, Haberstroh J, Walker UA. Time-dependent and tissue-specific accumulation of mtDNA and respiratory chain defects in chronic doxorubicin cardiomyopathy. *Circulation.* 2003; 108:2423–2429.
8. Ide T, Tsutsui H, Kinugawa S, Utsumi H, Kang D, Hattori N, Uchida K, Arimura K, Egashira K, Takeshita A. Mitochondrial electron transport complex I is a potential source of oxygen free radicals in the failing myocardium. *Circ Res.* 1999;85:357–363.
9. Ide T, Tsutsui H, Hayashidani S, Kang D, Suematsu N, Nakamura K, Utsumi H, Hamasaki N, Takeshita A. Mitochondrial DNA damage and dysfunction associated with oxidative stress in failing hearts after myocardial infarction. *Circ Res.* 2001;88:529–535.
10. Parisi MA, Clayton DA. Similarity of human mitochondrial transcription factor 1 to high mobility group proteins. *Science.* 1991;252:965–969.
11. Larsson NG, Wang J, Wilhelmsson H, Oldfors A, Rustin P, Lewandoski M, Barsh GS, Clayton DA. Mitochondrial transcription factor A is necessary for mtDNA maintenance and embryogenesis in mice. *Nat Genet.* 1998;18:231–236.
12. Li H, Wang J, Wilhelmsson H, Hansson A, Thoren P, Duffy J, Rustin P, Larsson NG. Genetic modification of survival in tissue-specific knockout mice with mitochondrial cardiomyopathy. *Proc Natl Acad Sci U S A.* 2000;97:3467–3472.
13. Wang J, Wilhelmsson H, Graff C, Li H, Oldfors A, Rustin P, Bruning JC, Kahn CR, Clayton DA, Barsh GS, Thoren P, Larsson NG. Dilated cardiomyopathy and atrioventricular conduction blocks induced by heart-specific inactivation of mitochondrial DNA gene expression. *Nat Genet.* 1999;21:133–137.
14. Kanazawa A, Nishio Y, Kashiwagi A, Inagaki H, Kikkawa R, Horiike K. Reduced activity of mtTFA decreases the transcription in mitochondria isolated from diabetic rat heart. *Am J Physiol.* 2002;282:E778–E785.
15. Garnier A, Fortin D, Delomenie C, Momken I, Veksler V, Ventura-Clapier R. Depressed mitochondrial transcription factors and oxidative capacity in rat failing cardiac and skeletal muscles. *J Physiol.* 2003;551: 491–501.
16. Niwa H, Yamamura K, Miyazaki J. Efficient selection for high-expression transfectants with a novel eukaryotic vector. *Gene.* 1991;108: 193–199.
17. Shiomi T, Tsutsui H, Hayashidani S, Suematsu N, Ikeuchi M, Wen J, Ishibashi M, Kubota T, Egashira K, Takeshita A. Pioglitazone, a peroxisome proliferator–activated receptor-gamma agonist, attenuates left ventricular remodeling and failure after experimental myocardial infarction. *Circulation.* 2002;106:3126–3132.
18. Shiomi T, Tsutsui H, Matsusaka H, Murakami K, Hayashidani S, Ikeuchi M, Wen J, Kubota T, Utsumi H, Takeshita A. Overexpression of glutathione peroxidase prevents left ventricular remodeling and failure after myocardial infarction in mice. *Circulation.* 2004;109:544–549.
19. Moraes CT, Shanske S, Tritschler HJ, Aprille JR, Andreetta F, Bonilla E, Schon EA, DiMauro S. mtDNA depletion with variable tissue expression: a novel genetic abnormality in mitochondrial diseases. *Am J Hum Genet.* 1991;48:492–501.
20. Lewis W, Gonzalez B, Chomyn A, Papoian T. Zidovudine induces molecular, biochemical, and ultrastructural changes in rat skeletal muscle mitochondria. *J Clin Invest.* 1992;89:1354–1360.
21. Marin-Garcia J, Goldenthal MJ. Mitochondrial cardiomyopathy: molecular and biochemical analysis. *Pediatr Cardiol.* 1997;18:251–260.
22. Scarpulla RC. Nuclear activators and coactivators in mammalian mitochondrial biogenesis. *Biochim Biophys Acta.* 2002;1576:1–14.
23. Inagaki H, Kitano S, Lin KH, Maeda S, Saito T. Inhibition of mitochondrial gene expression by antisense RNA of mitochondrial transcription factor A (mtTFA). *Biochem Mol Biol Int.* 1998;45:567–573.
24. Montoya J, Perez-Martos A, Garstka HL, Wiesner RJ. Regulation of mitochondrial transcription by mitochondrial transcription factor A. *Mol Cell Biochem.* 1997;174:227–230.
25. Ekstrand MI, Falkenberg M, Rantanen A, Park CB, Gaspari M, Hultenby K, Rustin P, Gustafsson CM, Larsson NG. Mitochondrial transcription factor A regulates mtDNA copy number in mammals. *Hum Mol Genet.* 2004;13:935–944.
26. Alam TI, Kanki T, Muta T, Ukaji K, Abe Y, Nakayama H, Takio K, Hamasaki N, Kang D. Human mitochondrial DNA is packaged with TFAM. *Nucleic Acids Res.* 2003;31:1640–1645.
27. Takamatsu C, Umeda S, Ohsato T, Ohno T, Abe Y, Fukuoh A, Shinagawa H, Hamasaki N, Kang D. Regulation of mitochondrial D-loops by transcription factor A and single-stranded DNA-binding protein. *EMBO Rep.* 2002;3:451–456.
28. Russell LK, Mansfield CM, Lehman JJ, Kovacs A, Courtois M, Saffitz JE, Medeiros DM, Valencik ML, McDonald JA, Kelly DP. Cardiac-specific induction of the transcriptional coactivator peroxisome proliferator-activated receptor gamma coactivator-1alpha promotes mitochondrial biogenesis and reversible cardiomyopathy in a developmental stage-dependent manner. *Circ Res.* 2004;94:525–533.
29. Lin J, Wu H, Tarr PT, Zhang CY, Wu Z, Boss O, Michael LF, Puigserver P, Isotani E, Olson EN, Lowell BB, Bassel-Duby R, Spiegelman BM. Transcriptional co-activator PGC-1 alpha drives the formation of slow-twitch muscle fibres. *Nature.* 2002;418:797–801.
30. Wu Z, Puigserver P, Andersson U, Zhang C, Adelmant G, Mootha V, Troy A, Cinti S, Lowell B, Scarpulla RC, Spiegelman BM. Mechanisms controlling mitochondrial biogenesis and respiration through the thermogenic coactivator PGC-1. *Cell.* 1999;98:115–124.
31. Huss JM, Kelly DP. Nuclear receptor signaling and cardiac energetics. *Circ Res.* 2004;95:568–578.
32. Ventura-Clapier R, Garnier A, Veksler V. Energy metabolism in heart failure. *J Physiol.* 2004;555:1–13.
33. Anan R, Nakagawa M, Miyata M, Higuchi I, Nakao S, Suehara M, Osame M, Tanaka H. Cardiac involvement in mitochondrial diseases: a study on 17 patients with documented mitochondrial DNA defects. *Circulation.* 1995;91:955–961.
34. Corral-Debrinski M, Shoffner JM, Lott MT, Wallace DC. Association of mitochondrial DNA damage with aging and coronary atherosclerotic heart disease. *Mutat Res.* 1992;275:169–180.
35. Arbustini E, Diegoli M, Fasani R, Grasso M, Morbini P, Banchieri N, Bellini O, Dal Bello B, Pilotto A, Magrini G, Campana C, Fortina P, Gavazzi A, Narula J, Vigano M. Mitochondrial DNA mutations and mitochondrial abnormalities in dilated cardiomyopathy. *Am J Pathol.* 1998;153:1501–1510.

Synergistic enhancement of TRAIL- and tumor necrosis factor α–induced cell death by a phenoxazine derivative

Keiichi Hara,[1] Mayumi Okamoto,[1] Toshihiko Aki,[2] Hideo Yagita,[3] Hirotoshi Tanaka,[4] Yoichi Mizukami,[2] Hiroshi Nakamura,[4] Akio Tomoda,[5] Naotaka Hamasaki,[1] and Dongchon Kang[1]

[1]Department of Clinical Chemistry and Laboratory Medicine, Kyushu University Graduate School of Medical Sciences, Fukuoka; [2]Center for Gene Research, Yamaguchi University, Yamaguchi; [3]Department of Immunology, Juntendo University School of Medicine; [4]Division of Clinical Immunology, Advanced Clinical Research Center, Institute of Medical Science, University of Tokyo; and [5]Department of Biochemistry and Research Institute of Immunological Treatment, Tokyo Medical University, Tokyo, Japan

Abstract

2-Amino-4,4α-dihydro-4α,7-dimethyl-3H-phenoxazine-3-one (Phx-1) has been developed as a novel phenoxazine derivative having an anticancer activity on a variety of cancer cell lines as well as transplanted tumors in mice with minimal toxicity to normal cells. We examined the effects of Phx-1 on Jurkat cells, a human T cell line. Phx-1 inhibited proliferation of the cells in a dose-dependent manner but hardly induced cell death, suggesting that Phx-1 acts primarily as an antiproliferative reagent but not as a cytocidal drug. Phx-1 enhanced tumor necrosis factor–related apoptosis-inducing ligand (TRAIL)-induced apoptotic cell death about 100-fold. Tumor necrosis factor α, which alone does not induce cell death of Jurkat cells, caused apoptosis in combination with Phx-1. These enhancements of cell death were not due to up-regulation of the death receptors. Phx-1 decreased serum-induced phosphorylation of Akt, a kinase involved in cell proliferation and survival, and inhibited complex III of mitochondrial respiratory chain. Considering that both TRAIL and Phx-1 have only marginal cytotoxicity to most normal cells, Phx-1 may provide an ideal combination for cancer therapy with TRAIL. [Mol Cancer Ther 2005;4(7):1121–7]

Received 3/10/05; revised 4/13/05; accepted 4/29/05.

Grant support: Supported in part by the Naito Foundation and Grants-in-Aid for Scientific Research from the Ministry of Education, Science, Technology, Sports, and Culture of Japan.

The costs of publication of this article were defrayed in part by the payment of page charges. This article must therefore be hereby marked advertisement in accordance with 18 U.S.C. Section 1734 solely to indicate this fact.

Requests for reprints: Dongchon Kang, Department of Clinical Chemistry and Laboratory Medicine, Kyushu University Graduate School of Medical Sciences, 3-1-1 Maidashi, Higashi, Fukuoka 812-8582, Japan. Phone: 81-92-642-5749; Fax: 81-92-642-5772. E-mail: kang@mailserver.med.kyushu-u.ac.jp

Introduction

Tumor necrosis factor (TNF)–related apoptosis-inducing ligand (TRAIL), a member of the TNF family, interacts with the death receptors, DR4 and DR5, and initiates a caspase-mediated cascade resulting in apoptosis. TRAIL induces apoptosis in a wide range of tumor cell lines, but not in most normal cells. Thus, TRAIL may represent a suitable ligand as an anticancer therapeutic drug (1). Sensitivity to TRAIL is enhanced by combination treatments with either chemotherapeutic agents or irradiation (2, 3). Almost all of the chemotherapeutic agents used in such combinations are also toxic to normal cells, and therefore it is important to find reagents that are not toxic to normal cells but synergize with TRAIL.

Actinomycin D, which shows a strong antitumor activity by intercalating DNA (4, 5), contains a phenoxazine structure. However, phenoxazines which have thus far been chemically synthesized have little water solubility, or hardly exert antitumor effects (6). Tomoda et al. have synthesized a novel water-soluble phenoxazine compound, 4α-dihydro-4α,7-dimethyl-3H-phenoxazine-3-one (Phx-1, Fig. 1; ref. 7). Phx-1 is produced by the reaction of 2-amino-5-methylphenol with human or bovine hemoglobin. Phx-1 inhibits the proliferation of a variety of cultured cell lines such as human epidermoid carcinoma cells (8), Meth A tumor cells (9), human lung carcinoma cell lines (10), leukemia cell lines K562, HL-60, and HAL-01 (11), human endometrial adenocarcinoma cell lines EN and KLE cells (12). In addition to the *in vitro* effects, Phx-1 also reduces the growth of tumor cells in mice that are transplanted with the cells (9, 11). As Phx-1 has an antitumor activity in a variety of tumor cells but little cytotoxicity to normal cells (9, 11), this compound may have a potential as a novel anticancer drug. This compound, unlike actinomycin D, does not intercalate DNA, and hence suppresses the proliferation of tumor cells in a manner distinct from actinomycin D. Currently, however, little is known of how Phx-1 acts on the tumor cells.

In this study, we found that the phenoxazine derivatives effectively enhanced the TRAIL- and TNFα-induced cell death, which may make this compound more promising as an antitumor drug.

Materials and Methods

Reagents

Phx-1 (13) and -2 (14) were synthesized and purified as described previously. TNFα was purchased from Sigma (St. Louis, MO). Purified TRAIL was kindly given by Myung-Shik Lee (Samsung Medical Center; ref. 15). Anti-human TNF receptor type I-biotin, anti-human TNF receptor type II-biotin, anti-human IGF receptor I-phycoerythrin, and streptavidin-phycoerythrin were from Becton Dickinson

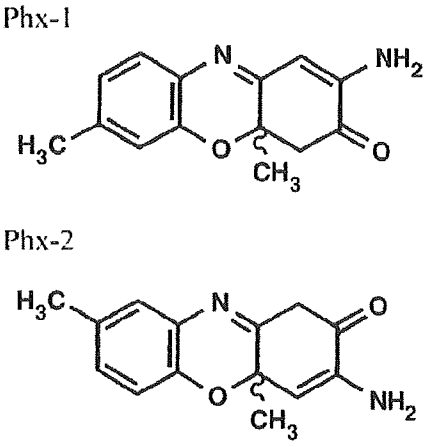

Figure 1. Structure of Phx-1 and Phx-2.

(Mountain View, CA). For detection of TRAIL receptors, biotin-labeled anti-DR4 (DJR1) and anti-DR5 (DJR2) mouse monoclonal antibodies were used (16). 3-(4,5-Dimethylthiazol-2-yl)-2,5-diphenyltetrazolium bromide and 2-(4-iodophenyl)-3-(4-nitrophenyl)-5-(2,4-disulfophenyl)-2H-tetrazolium monosodium salt were from Dojin (Kumamoto, Japan).

Cell Count

Jurkat cells, a human T cell leukemic cell line, were cultured in RPMI 1640 (Sigma) containing 10% fetal bovine serum (FBS) at 37°C under 95% air/5% CO_2. Jurkat cells (1×10^5 cells in 2 mL medium) were seeded onto a well of a six-well plate and grown in the presence or absence of Phx. An aliquot (10 μL) was taken at each day and viable cells that were not stained with a trypan blue dye were counted.

3-(4,5-Dimethylthiazol-2-yl)-2,5-diphenyltetrazolium bromide and 2-(4-iodophenyl)-3-(4-nitrophenyl)-5-(2,4-disulfophenyl)-2H-tetrazolium monosodium salt assays were done according to the manufacturer's instructions (Dojin). Briefly, 3×10^4 cells in 100 μL were plated into a 96-well plate and incubated with the indicated reagents for 24 hours. For the former, 50 μL of 5 mg/mL 3-(4,5-dimethylthiazol-2-yl)-2,5-diphenyltetrazolium bromide was added onto each well and the cells were incubated for another 4 hours. After removing the medium, the resulting insoluble dye was solubilized by adding 100 μL of DMSO. The absorbance was measured at 570 to 650 nm. For the latter, the medium was replaced by 100 μL of PBS and 10 μL of the 2-(4-iodophenyl)-3-(4-nitrophenyl)-5-(2,4-disulfophenyl)-2H-tetrazolium monosodium salt solution. The cells were incubated for another 1 hour. The absorbance was measured at 450 to 650 nm.

Phosphorylation of Protein Kinases

Jurkat cells were grown to 70% confluence in RPMI containing 10% FBS. After 48 hours incubation without serum, the cells were incubated for 30 minutes in RPMI without serum containing 50 μmol/L Phx-1 and then incubated with 10% FBS for the indicated time. The cells were washed with PBS twice and the total cell lysates were prepared (17). Eight micrograms of the lysates were used for detection of phosphorylation of protein kinases by immunoblotting: Akt with rabbit anti-Akt antibodies (Cell Signaling, Beverly, MA), phosphorylated Akt with rabbit anti-phospho-Ser^{473}-Akt antibodies (Cell Signaling), extracellular signal-regulated protein kinase (ERK) with rabbit anti-ERK2 (Santa Cruz, Santa Cruz, CA), phosphorylated ERK with mouse anti-phospho-ERK (E-4; Santa Cruz), p38 mitogen-activated protein kinase (p38MAPK) with rabbit anti-p38MAPK (Cell Signaling), and phosphorylated p38MAPK with rabbit anti-phospho-p38MAPK (Thr^{180}/Thr^{182}; Cell Signaling; ref. 18).

Mitochondrial Membrane Potential

The mitochondrial membrane potential was analyzed with JC-1, a lipophilic cationic fluorescence dye, using a mitochondrial membrane potential detection kit, MitoProbe (Molecular Probes, Eugene, OR). JC-1 enters mitochondria and changes its emission light from green (FL-1) to red (FL-2) as the mitochondrial membrane become more polarized. Jurkat cells were incubated with the indicated reagents for 24 hours, The cells were then washed with PBS, resuspended in RPMI/2% FBS containing 2.0 μmol/L JC-1 at 1×10^6 cells/mL for 30 minutes at 37°C. After washing with RPMI/2% FBS, the cells were resuspended in PBS and analyzed on a FACSCalibur flow cytometer (Becton Dickinson). Ten thousand events were recorded and analyzed with a CellQuest program (Becton Dickinson).

Apoptosis

After 24-hour incubation of Jurkat cells with the indicated reagents, binding of Annexin V-FITC and staining of propidium iodide were measured for assessment of early and late apoptosis, respectively, using an Annexin V-FITC apoptosis detection kit (BD Biosciences, Palo Alto, CA).

Cell Surface Receptors

After 12-hour incubation of Jurkat cells with the indicated reagents, the cells were washed once with PBS, resuspended in PBS/2% FBS containing the indicated phycoerythrin-labeled or biotin-labeled antibodies against cell surface receptors, and incubated for 45 minutes at 4°C. The cells were washed with PBS and incubated, if necessary, with the streptavidin-phycoerythrin. The fluorescence of phycoerythrin was analyzed on a FACSCalibur flow cytometer.

Mitochondrial Enzyme Activities

Activities of complex I (NADH-ubiquinone oxidoreducatse), complex II (succinate-ubiquinone oxidoreducatse), and complexes II and III (succinate-cytochrome *c* oxidoreductase) were measured as described by Trounce et al. (19). Mitochondria were prepared from Jurkat cells by differential centrifugation and following sucrose density gradient separation as described previously (20).

Results

Effects of Phx on Proliferation of Human Leukemia T Cells

We first examined if Phx-1 inhibits proliferation of Jurkat cells. Jurkat cells were grown in medium containing 0, 20,

50, and 100 μmol/L Phx-1. The cells that were not stained with a trypan blue dye were directly counted. Phx inhibited the cell proliferation in a dose-dependent manner (Fig. 2A). Phx-1 strongly inhibited the cell growth at 50 μmol/L and completely inhibited at 100 μmol/L. Most cells were trypan blue–negative, i.e., alive at 50 μmol/L for 3 days. Less than 2% of the dead cells were trypan blue–positive on day 1 even in the presence of 100 μmol/L Phx-1, suggesting that Phx-1 is primarily antiproliferative but not cytocidal on Jurkat cells. More than 50% of the cells were trypan blue–positive at day 3 in the presence of 100 μmol/L Phx-1.

Phx-1 down-regulates IgM receptors on B cells (21). To see if the inhibition of cell growth is related to the decrease in cell surface receptors, the amounts of various cell surface receptors of Jurkat were examined. IGF receptors, which are involved in the proliferation of Jurkat cells (22), are not affected by Phx-1 (Fig. 2B). None of the other receptors examined (CD2, CD3, CD7, CD8, and CXCR4) were changed by Phx-1 (results not shown). These results suggest that the antiproliferative effect of Phx-1 is not exerted by the modulation of cell surface receptors or differentiation.

Phosphorylation of Akt by serum addition, a protein kinase involved in cell survival and proliferation signals, was strongly inhibited at 50 μmol/L Phx-1 (Fig. 2C) and also at 20 μmol/L to a similar extent (results not shown). On the other hand, phosphorylation of ERK, another protein kinase involved in cell survival and proliferation signals, was not affected (Fig. 2D, *top*). Phosphorylation of p38MAPK, which is mainly located downstream of inflammatory cytokine receptors, was barely changed by the serum addition or by Phx-1 (Fig. 2D, *bottom*). These results are consistent with a recent report that Phx-1 inhibited antigen-induced phosphorylation of Akt but not that of ERK or p38MAPK in B cells (23).

Synergistic Effects on TRAIL-Induced Cell Death

Next, we examined if Phx-1 affects cytotoxicity of TRAIL. Jurkat cells were incubated with various concentrations of TRAIL for 24 hours and then the living cell number was estimated by a 3-(4,5-dimethylthiazol-2-yl)-2,5-diphenyltetrazolium bromide assay that is based on the activity of mitochondrial succinate dehydrogenase. The number of living cells decreased in a dose-dependent fashion (Fig. 3A, *top*). Most cells died at 1,000 ng/mL TRAIL. When the cells were coincubated with TRAIL and 50 μmol/L Phx-1, cell death was enhanced by two orders of magnitude; most cells died at 10 ng/mL TRAIL in the presence of 50 μmol/L Phx-1. Phx-1 alone decreased the number of living cells to about 70% of the control (Fig. 3A, *top*) but we observed essentially no trypan blue–positive cells as described above. To adjust this antiproliferative effect, we expressed the cell number as relative changes (Fig. 3A, *bottom*). The

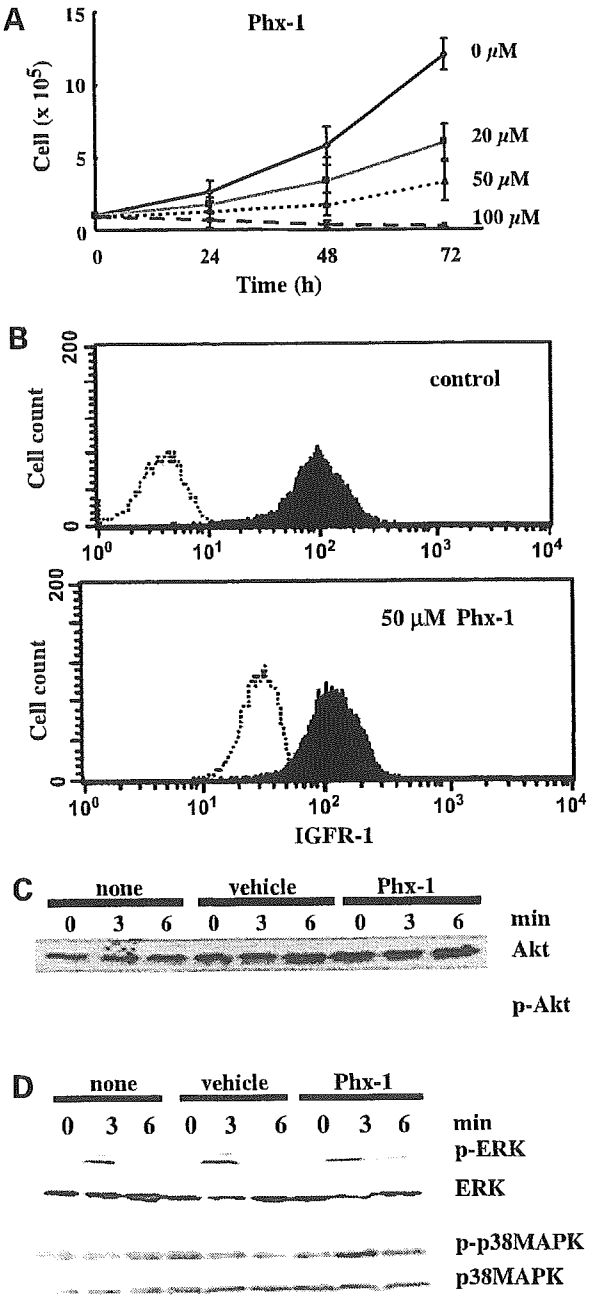

Figure 2. Effects on growth of Jurkat cells. **A**, Jurkat cells were cultured in the presence of various concentrations of Phx-1. The trypan blue–negative viable cells were counted daily. *Bars*, 1 SD from 3 independent experiments. **B**, expression of IGF receptor I (IGFR-I). After 24 h of incubation with 50 μmol/L Phx-1, the cells were incubated with (*solid line*) or without (*broken line*) biotin-labeled anti-IGF receptor I and then incubated with FITC-labeled streptavidin. The incubation with Phx increased nonspecific fluorescent signals due to fluorescence of Phx-1 per se (compare *broken lines, top* and *bottom*). The apparent increase in specific signals after Phx incubation (compare *solid lines, top* and *bottom*) exactly corresponded with the increase in the nonspecific signals, indicating that there is no increase in expression of IGFR-I. **C**, phosphorylation of Akt. Jurkat cells were preincubated for 30 min in the FBS-free medium containing 50 μmol/L Phx-1 and then incubated with 10% FBS for the indicated time. The total cell lysates were used for the detection of Akt and phosphorylated Akt (p-Akt) by immunoblotting. **D**, phosphorylation of ERK and p38MAPK was examined as in (**C**). *p-ERK*, phosphorylated ERK; *p-p38MAPK*, phosphorylated p38MAPK.

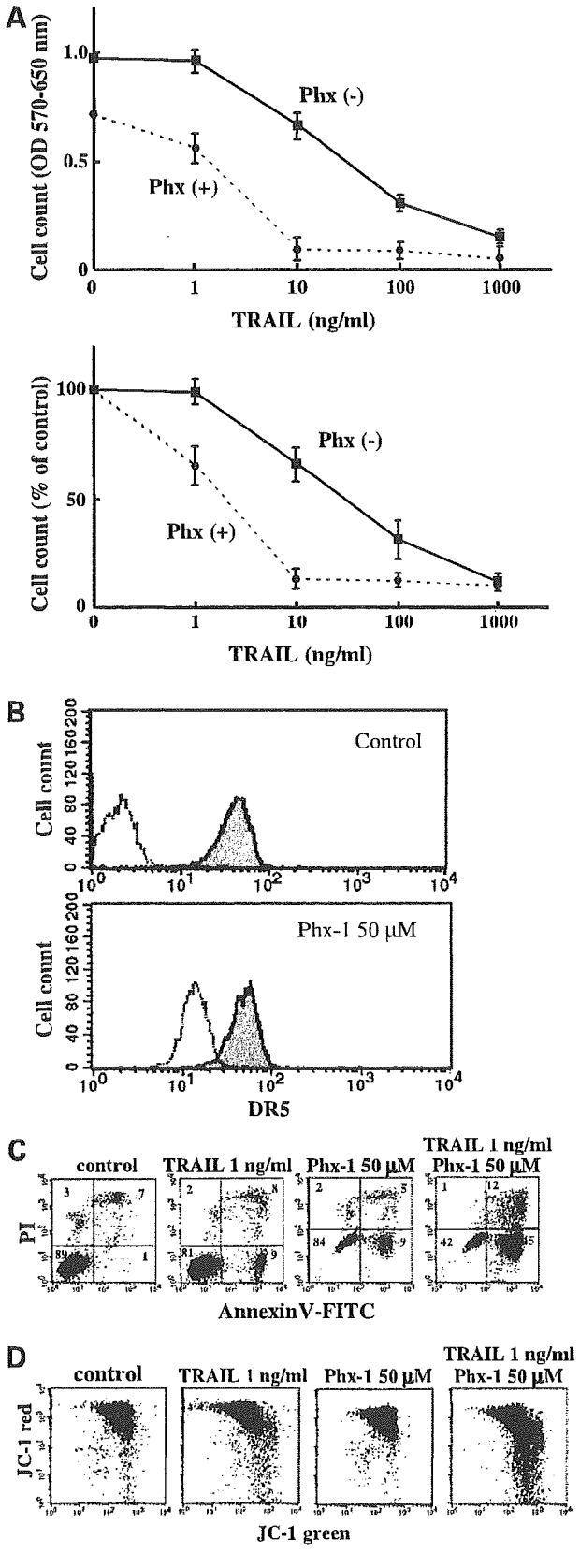

marked enhancement of cell death with Phx-1 was clearly shown in this method of presentation. A TRAIL receptor, DR5, was not increased by Phx-1 (Fig. 3B), suggesting that this enhancement of cell death was not mediated by the increase in DR5. Another TRAIL receptor, DR4 was not expressed on the Jurkat cells (results not shown).

Then, we examined by estimating Annexin V-binding–positive cells if the cell death is apoptotic. In consistence with the results of trypan blue staining, 50 μmol/L Phx-1 alone marginally increased the Annexin V-positive cells (Fig. 3C). The combination of TRAIL and Phx-1 markedly enhanced the Annexin V-positive cells. These results suggest that Phx-1 potentiated the apoptotic effect of TRAIL.

TRAIL or Phx-1 alone hardly decreased mitochondrial membrane potential but their combination decreased it (Fig. 3D), suggesting that the apoptosis is mediated at least in part by mitochondrial dysfunction.

Effects on TNFα-Mediated Cell Death

It is well-known that TNFα alone, a death receptor–mediated apoptotic factor, hardly induced cell death of Jurkat cells (Fig. 4A). TNFα-induced cell death in combination with Phx-1 (Fig. 4A), whereas TNFα receptor 1 was not up-regulated by Phx-1 on the cell surface (Fig. 4B). The TNFα receptor 2 was not expressed on the Jurkat cells (results not shown). This cell death was apoptotic because Annexin V-positive cells were increased by the combinational incubation (Fig. 4C). The mitochondrial membrane potential was also decreased by the incubation with TNFα and Phx-1 (Fig. 4D).

Effects on Respiratory Chain Activities

Phx-1 inhibited the complex II and III (succinate-cytochrome *c* oxidoreductase) activity of isolated mitochondria of Jurkat cells (Fig. 5A). The activity was decreased to about 15% of the control at 200 μmol/L. The activity of complex II (succinate-ubiquinone oxidoreductase) was decreased to about 75% of the control with 200 μmol/L Phx-1 (Fig. 5A), suggesting that Phx-1 mainly inhibited complex III (ubiquinone-cytochrome *c* oxidoreductase). The activity of complex I (NADH-ubiquinone oxidoreductase) was not inhibited with Phx-1 (results not shown).

To see the involvement of the respiratory chain, we examined mitochondrial DNA-less cells (Fig. 5B). TRAIL hardly induced the cell death of normal 143B cells derived from human osteosarcoma even at 1,000 ng/mL. Phx-1 did not show any synergistic effects on it. However, a mtDNA-less (ρ0) cell line of the 143B, which is devoid of the

Figure 3. Synergistic effects of Phx-1 and TRAIL. Jurkat cells were incubated with the indicated reagents for 24 h. **A,** the cell number was estimated by a 3-(4,5-dimethylthiazol-2-yl)-2,5-diphenyltetrazolium bromide assay. Three independent experiments were done. *Top,* one representative experiment of the three independent experiments. *Points,* mean; *bars,* 1 SD. *Bottom,* the amount of cells at day 0 was expressed as 100%. *Points,* mean; *bars,* ± SD. **B,** the amount of cell surface DR5 was analyzed as in Fig. 2B. **C,** early (Annexin V-positive) and late (propidium iodide–positive) apoptotic cells were analyzed. The value in each compartment indicates the percentage of distribution of cells. **D,** the mitochondrial membrane potential (*JC-1 red*) was estimated.

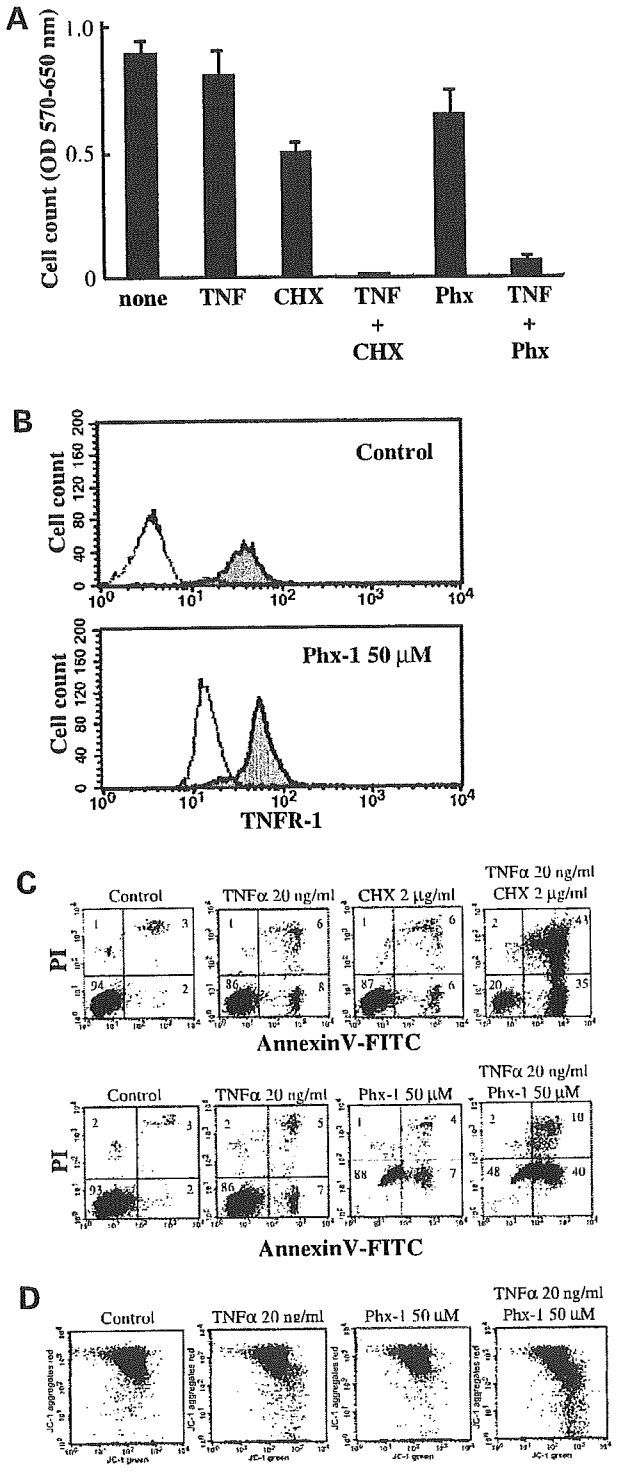

Figure 4. Synergistic effects of Phx-1 and TNFα. **A,** Jurkat cells were incubated with the indicated reagents for 24 h and then cell numbers were measured as in Fig. 3A. *Columns*, mean; *bars*, ± SD. *TNF*, TNFα (20 ng/mL); *CHX*, cycloheximide (2 μg/mL); *Phx*, Phx-1 (50 μmol/L). **B,** the cell surface TNF receptor 1 (*TNFR-1*) was measured. **C,** the apoptotic cells were estimated as in Fig. 3C. **D,** the mitochondrial membrane potential was estimated as in Fig. 3D.

respiratory activity, showed a weak sensitivity to TRAIL. Phx-1 enhanced this cell death by two orders of magnitude; the living cells were decreased with 10 ng/mL TRAIL plus 50 μmol/L Phx-1 more strongly than with 1,000 ng/mL TRAIL alone (Fig. 5B), suggesting that the cell death enhancement by Phx-1 does not necessarily require the activity of the respiratory chain.

Discussion

Tomoda et al. have synthesized a novel phenoxazine derivative, Phx-1, which shows antitumor effects. Phx could be a promising anticancer drug owing to its minimal side effects. In this work, we have shown that Phx-1 has an antiproliferative activity with little cytocidal activity, suggesting that the primary action of Phx-1 on Jurkat cells is antiproliferation. Higher doses of Phx-1 and longer incubation caused cell death. 3-Amino-1,4α-dihydro-4α,8-dimethyl-2H-phenoxazine-2-one (Phx-2, Fig. 1), which is a chemical isomer of Phx-1, at 100 μmol/L showed essentially the same effects on cell proliferation, TRAIL- and TNFα-induced apoptosis as did Phx-1 at 50 μmol/L (results not shown).

Under the conditions where Phx-1 showed only antiproliferative effects (Figs. 2A and 3C), Phx-1 markedly enhanced TRAIL-induced cell death of Jurkat cells (Fig. 3A). In addition, similar to cycloheximide, Phx-1 induced cell death with TNFα (Fig. 4A). Because these cell deaths were apoptotic, Phx-1 may potentiate the apoptotic death signals. This hypothesis is compatible with the experiments of 143B cells. The respiration-competent 143B cells were completely resistant to TRAIL, whereas the respiration-incompetent mtDNA-less (ρ0) 143B cells acquired weak sensitivity. Phx-1 could not induce cell death of respiration-competent 143B cells even in the presence of 1,000 ng/mL TRAIL but enhanced the cell death of the respiration-incompetent 143B cells (Fig. 5B), supporting the idea that Phx-1 hardly elicits apoptotic signals but strongly augments the death signals once elicited. This augmentation may occur within a cell because there was no up-regulation of cell surface receptors such as TNFα and TRAIL receptors. Phx-1 inhibited the phosphorylation of Akt, a protein kinase that can work both for cell proliferation and cell survival. It is reported that Akt-inhibition enhances TRAIL-induced apoptosis in glioma cells (24), whereas Akt-overexpression can inhibit TRAIL-induced apoptosis (25). Thus, the inhibition of the Akt pathway may contribute to the antiproliferation as well as to the cell death enhancement by Phx-1 although it is not yet certain to what extent the inhibition of Akt contributes to the two actions of Phx-1.

2-Methoxyestradiol, a naturally occurring metabolite of estradiol, also enhances cell death by TRAIL (26). This enhancement is exerted at least in part by increasing the expression of DR5 and by suppressing the HIF-1α (26). Phx-1 did not increase the expression of DR5 (Fig. 3B). Overexpression of constitutive active HIF-1α in Jurkat cells (27) did not affect the cell death with TRAIL plus Phx-1 (results not shown). Thus, Phx-1 may enhance the TRAIL-induced cell death in a different manner from 2-methoxyestradiol.

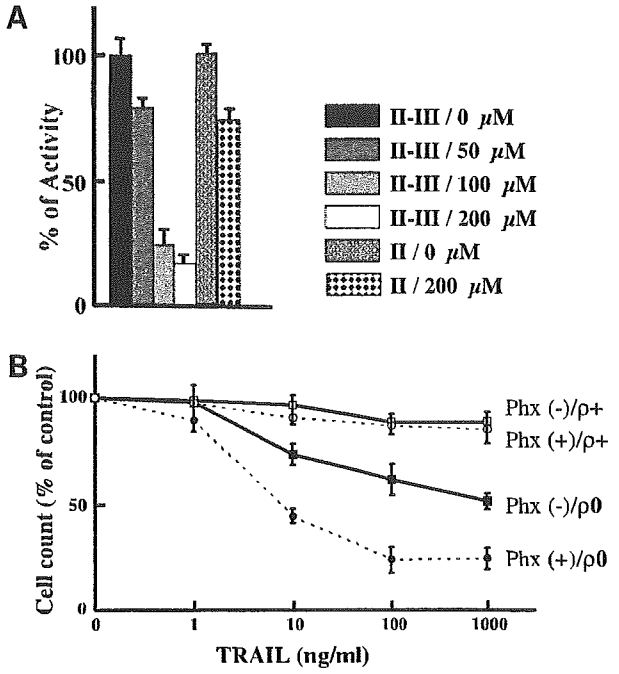

Figure 5. Respiratory chain. **A,** activities of complex II and complexes II and III. Mitochondria were prepared from Jurkat cells. The mitochondria were incubated with various concentrations of Phx-1 at 37°C for 5 min and then activities of complex II and complexes II and III were measured. *Columns*, mean; *bars*, ± SD. **B,** effects on 143B ρ0 cells. The wild-type 143B (ρ+) and mtDNA-less 143B (ρ0) cells were incubated for 24 h with the indicated reagents. The cell number was estimated by a 2-(4-iodophenyl)-3-(4-nitrophenyl)-5-(2,4-disulfophenyl)-2H-tetrazolium monosodium salt assay in which lactate dehydrogenase activity is measured because ρ0 cells are respiration-incompetent. *Bars*, 1 SD. *Phx (+)*, 50 μmol/L Phx-1.

The inhibitor of apoptosis protein family (IAP) inhibits caspase-3, which is a major final executing caspase of apoptosis, and thus negatively regulates apoptosis. In recent reports, several small molecule antagonists of IAPs potentiated TRAIL-induced cell death (28–30). TNFα-elicited death signaling may be antagonized by IAPs when TNFα is applied alone (31). Cycloheximide restores the TNFα-induced cell death probably by suppressing this IAP-mediated inhibition of apoptosis because second mitochondria-derived activator of caspases (Smac), an inhibitor of IAPs, substituted cycloheximide for the TNFα-induced cell death (29). Considering that Phx-1 also caused TNFα-induced apoptosis instead of cycloheximide, Phx-1 may act on a pathway leading to suppression of IAPs, for example by enhancing the release of Smac from mitochondria. In this context, it should be noted that Phx-1 inhibits complex III. This inhibition could modulate mitochondrial functions. In fact, Phx-1 synergistically decreased the mitochondrial membrane potential in combination with TRAIL or TNFα. The inhibition of the respiratory chain may contribute to the antiproliferation as well as apoptosis enhancement, at least in respiration-competent cells, although mitochondrial respiration is not necessarily required for the enhancement of apoptosis.

Higher concentrations of Phx-1 are required for *in vitro* inhibition of the respiratory chain than for that of the proliferation or phosphorylation of Akt. One possibility is that Phx-1 may accumulate in mitochondria *in vivo*. Cationic and lipophilic reagents are concentrated in mitochondria *in vivo* due to the mitochondrial inside-negative membrane potential. Phx-1 has an amino base on an aromatic ring (Fig. 1) and so might be cationic and lipophilic in a cell to some extent. Another possibility is that Phx-1 is metabolized in a cell and converted to a more effective substance. 1-Methyl-4-phenyl-1,2,3,6-tetrahydropyridine, which produces an experimental model of Parkinson's disease in animals, is a good example of the above situation. 1-Methyl-4-phenyl-1,2,3,6-tetrahydropyridine is oxidized in glial cells to 1-methyl-4-phenylpyridinium ion. This metabolite is concentrated in mitochondria due to its cationic and lipophilic nature and then inhibits the respiratory chain (32).

In conclusion, Phx-1 inhibited proliferation of Jurkat cells on its own and enhanced cell death in combination with TRAIL or TNFα. Phx-1 and its related compounds may be useful for an understanding of the regulation of TRAIL- and TNFα-induced apoptosis. Moreover, because TRAIL or Phx is not cytotoxic to most normal cells, their synergistic activation of apoptosis would provide an ideal combination for cancer therapy.

References

1. Yagita H, Takeda K, Hayakawa Y, Smyth MJ, Okumura K. TRAIL and its receptors as targets for cancer therapy. Cancer Sci 2004;95:777–83.

2. Shankar S, Srivastava RK. Enhancement of therapeutic potential of TRAIL by cancer chemotherapy and irradiation: mechanisms and clinical implications. Drug Resist Updat 2004;7:139–56.

3. Wajant H, Pfizenmaier K, Scheurich P. TNF-related apoptosis inducing ligand (TRAIL) and its receptors in tumor surveillance and cancer therapy. Apoptosis 2002;7:449–59.

4. Goldberg IH, Friedman PA. Specificity in the mechanism of action of antibiotic inhibitors of protein and nucleic acid synthesis. Pure Appl Chem 1971;28:499–524.

5. Wadkins RM, Jares-Erijman EA, Klement R, Rudiger A, Jovin TM. Actinomycin D binding to single-stranded DNA: sequence specificity and hemi-intercalation model from fluorescence and 1H NMR spectroscopy. J Mol Biol 1996;262:53–68.

6. Motohashi N, Mitscher LA, Meyer R. Potential antitumor phenoxazines. Med Res Rev 1991;11:239–94.

7. Tomoda A, Hamashima H, Arisawa M, Kikuchi T, Tezuka Y, Koshimura S. Phenoxazinone synthesis by human hemoglobin. Biochim Biophys Acta 1992;1117:306–14.

8. Ishida R, Yamanaka S, Kawai H, et al. Antitumor activity of 2-amino-4,4 α-dihydro-4 α, 7-dimethyl-3H-phenoxazine-3-one, a novel phenoxazine derivative produced by the reaction of 2-amino-5-methylphenol with bovine hemolysate. Anticancer Drugs 1996;7:591–5.

9. Mori H, Honda K, Ishida R, Nohira T, Tomoda A. Antitumor activity of 2-amino-4,4α-dihydro-4α, 7-dimethyl-3H-phenoxazine-3-one against Meth A tumor transplanted into BALB/c mice. Anticancer Drugs 2000;11:653–7.

10. Abe A, Yamane M, Tomoda A. Prevention of growth of human lung carcinoma cells and induction of apoptosis by a novel phenoxazinone, 2-amino-4,4α-dihydro-4α,7-dimethyl-3H-phenoxazine-3-one. Anticancer Drugs 2001;12:377–82.

11. Shimamoto T, Tomoda A, Ishida R, Ohyashiki K. Antitumor effects of a novel phenoxazine derivative on human leukemia cell lines *in vitro* and *in vivo*. Clin Cancer Res 2001;7:704–8.

12. Nakada T, Isaka K, Nishi H, et al. A novel phenoxazine derivative suppresses proliferation of human endometrial adenocarcinoma cell

lines, inducing G2M accumulation and apoptosis. Oncol Rep 2003;10: 1171 – 6.

13. Tomoda A, Arai S, Ishida R, Shimamoto T, Ohyashiki K. An improved method for the rapid preparation of 2-amino-4,4a-dihydro-4a,7-dimethyl-3H-phenoxazine-3-one, a novel antitumor agent. Bioorg Med Chem Lett 2001;11:1057 – 8.

14. Tomoda A, Arisawa M, Koshimura S. Oxidative condensation of 2-amino-4-methylphenol to dihydrophenoxazinone compound by human hemoglobin. J Biochem (Tokyo) 1991;110:1004 – 7.

15. Kim JY, Kim YH, Chang I, et al. Resistance of mitochondrial DNA-deficient cells to TRAIL: role of Bax in TRAIL-induced apoptosis. Oncogene 2002;21:3139 – 48.

16. Uno K, Inukai T, Kayagaki N, et al. TNF-related apoptosis-inducing ligand (TRAIL) frequently induces apoptosis in Philadelphia chromosome-positive leukemia cells. Blood 2003;101:3658 – 67.

17. Mizukami Y, Kobayashi S, Uberall F, Hellbert K, Kobayashi N, Yoshida K. Nuclear mitogen-activated protein kinase activation by protein kinase cζ during reoxygenation after ischemic hypoxia. J Biol Chem 2000;275: 19921 – 7.

18. Mizukami Y, Okamura T, Miura T, et al. Phosphorylation of proteins and apoptosis induced by c-Jun N-terminal kinase 1 activation in rat cardiomyocytes by H(2)O(2) stimulation. Biochim Biophys Acta 2001; 1540:213 – 20.

19. Trounce IA, Kim YL, Jun AS, Wallace DC. Assessment of mitochondrial oxidative phosphorylation in patient muscle biopsies, lymphoblasts, and transmitochondrial cell lines. Methods Enzymol 1996;264:484 – 509.

20. Kang D, Nishida J, Iyama A, et al. Intracellular localization of 8-oxo-dGTPase in human cells, with special reference to the role of the enzyme in mitochondria. J Biol Chem 1995;270:14659 – 65.

21. Gao S, Takano T, Sada K, et al. A novel phenoxazine derivative suppresses surface IgM expression in DT40 B cell line. Br J Pharmacol 2002;137:749 – 55.

22. Baier TG, Jenne EW, Blum W, Schonberg D, Hartmann KK. Influence of antibodies against IGF-I, insulin or their receptors on proliferation of human acute lymphoblastic leukemia cell lines. Leuk Res 1992;16:807 – 14.

23. Enoki E, Sada K, Qu X, et al. The phenoxazine derivative Phx-1 suppresses IgE-mediated degranulation in rat basophilic leukemia RBL-2H3 cells. J Pharmacol Sci 2004;94:329 – 33.

24. Puduvalli VK, Sampath D, Bruner JM, Nangia J, Xu R, Kyritsis AP. TRAIL-induced apoptosis in gliomas is enhanced by Akt-inhibition and is independent of JNK activation. Apoptosis 2005;10:233 – 43.

25. Chen X, Thakkar H, Tyan F, et al. Constitutively active Akt is an important regulator of TRAIL sensitivity in prostate cancer. Oncogene 2001;20:6073 – 83.

26. Mooberry SL. Mechanism of action of 2-methoxyestradiol: new developments. Drug Resist Updat 2003;6:355 – 61.

27. Makino Y, Nakamura H, Ikeda E, et al. Hypoxia-inducible factor regulates survival of antigen receptor-driven T cells. J Immunol 2003; 171:6534 – 40.

28. Schimmer AD, Welsh K, Pinilla C, et al. Small-molecule antagonists of apoptosis suppressor XIAP exhibit broad antitumor activity. Cancer Cell 2004;5:25 – 35.

29. Li L, Thomas RM, Suzuki H, De Brabander JK, Wang X, Harran PG. A small molecule Smac mimic potentiates TRAIL- and TNFα-mediated cell death. Science 2004;305:1471 – 4.

30. Rosato RR, Dai Y, Almenara JA, Maggio SC, Grant S. Potent antileukemic interactions between flavopiridol and TRAIL/Apo2L involve flavopiridol-mediated XIAP downregulation. Leukemia 2004;18: 1780 – 8.

31. Wrzesien-Kus A, Smolewski P, Sobczak-Pluta A, Wierzbowska A, Robak T. The inhibitor of apoptosis protein family and its antagonists in acute leukemias. Apoptosis 2004;9:705 – 15.

32. Singer TP, Ramsay RR. Mechanism of the neurotoxicity of MPTP. An update. FEBS Lett 1990;274:1 – 8.

American Journal of Epidemiology

Vol. 161, No. 4
Printed in U.S.A.
DOI: 10.1093/aje/kwi049

Dietary Patterns and Colorectal Adenomas in Japanese Men

The Self-Defense Forces Health Study

Tetsuya Mizoue[1], Taiki Yamaji[1], Shinji Tabata[1,2], Keizo Yamaguchi[1,3], Eiichi Shimizu[3], Masamichi Mineshita[3], Shinsaku Ogawa[2], and Suminori Kono[1]

[1] Department of Preventive Medicine, Faculty of Medical Sciences, Kyushu University, Higashiku, Fukuoka, Japan.
[2] Self-Defense Forces Fukuoka Hospital, Fukuoka, Japan.
[3] Self-Defense Forces Kumamoto Hospital, Kumamoto, Japan.

Received for publication July 7, 2004; accepted for publication September 10, 2004.

The role of dietary patterns in colorectal carcinogenesis remains unclear in Asian populations. Using 1999–2002 data, the authors investigated the association between dietary patterns and colorectal adenomas in 1,341 Japanese men who underwent total colonoscopy. Information about diet was obtained using a 74-item food frequency questionnaire prior to the colonoscopy. Three dietary patterns were generated by factor analysis: 1) a high-dairy, high-fruit and -vegetable, high-starch, low-alcohol pattern; 2) an "animal food" pattern; and 3) a Japanese pattern. Logistic regression analysis was used to estimate the odds ratio of having colorectal adenomas with the adjustment for potential confounding variables including body mass index, smoking, alcohol, and leisure-time physical activities. A significant inverse association was found for the high-dairy, high-fruit and -vegetable, high-starch, low-alcohol pattern; the odds ratios for the second, third, and fourth quartiles were 0.97 (95% confidence interval: 0.70, 1.36), 0.71 (95% confidence interval: 0.50, 1.01), and 0.62 (95% confidence interval: 0.43, 0.90), respectively, compared with the lowest (p_{trend} = 0.003). Similar associations were observed for larger adenomas or for each subsite of the colorectum. The Japanese and "animal food" patterns were not clearly associated with colorectal adenomas. A dietary pattern including greater consumption of dairy products and fruits and vegetables with low alcohol consumption may be associated with decreased risk of colorectal adenomas.

adenoma; cross-sectional studies; diet

Abbreviation: DFSA, high-dairy, high-fruit and -vegetable, high-starch, low-alcohol (dietary pattern).

Colorectal cancer is a major cause of cancer deaths in developed countries. Geographic and time-trend analyses, as well as migrant studies, strongly suggest that environmental factors, especially diet, play an important role in the pathogenesis of colorectal cancer (1–3). However, analytical epidemiologic studies have yielded conflicting findings; for example, a body of evidence suggesting a protective role of vegetables or dietary fiber (4) has been either challenged (5–8) or supported (9, 10) by recent large-scale studies. In Japan, colorectal cancer mortality has markedly increased over the last several decades (11) and is now among the highest levels in the world (12). Time-trend analysis has suggested that decreased consumption of dietary fibers (13) or grains (14) may account for the increase in mortality. Yet it is largely unknown which lifestyle changes associated with Westernization or modernization have contributed to the rapid increase of colorectal cancer in Japan, or whether the traditional Japanese diet protects against this type of cancer.

Analysis of dietary patterns has recently drawn a great deal of attention as a method of investigating the role of foods or nutrients in studies of chronic diseases. Approaches of this sort, dealing with a combination of several foods, can overcome problems arising from close intercorrelation and potential effect modifications among numerous foods or nutrients (15). Factor-analysis studies of Western populations have suggested that a certain dietary pattern may be

Reprint requests to Dr. Tetsuya Mizoue, Department of Preventive Medicine, Faculty of Medical Sciences, Kyushu University, 3-1-1, Maidashi, Higashiku, Fukuoka 812-8582, Japan (e-mail: mizoue@phealth.med.kyushu-u.ac.jp).

predictive of colorectal cancer risk (16–18). Dietary patterns generated by factor analysis, however, are sample specific and may not be applicable to populations having different dietary cultures. While having adopted a Western-style diet, many Japanese still consume large amounts of traditional foods, including rice, fish, and soybean products (19). Thus, dietary patterns among Japanese may differ considerably from those among Western populations.

The aim of the present study was therefore to investigate dietary patterns in relation to the risk of colorectal adenoma, a precursor of colorectal cancer (20, 21), using data from preretirement check-ups among male Self-Defense Forces officials in Japan.

MATERIALS AND METHODS

Study setting

The data used were derived from the Self-Defense Forces Health Study, a cross-sectional survey of male Self-Defense Forces officials who participated in a preretirement health examination at two hospitals (Fukuoka and Kumamoto) in Japan. The study procedure has been described elsewhere (22, 23). In short, all officials undergo a comprehensive health examination before retirement; total colonoscopy is included as a routine procedure. Study questionnaires about health-related lifestyles were distributed prior to colonoscopy to male examinees on the first day of hospital admission for examination. Research assistants checked the questionnaire for unanswered questions and apparently inconsistent answers and, if necessary, sought clarification from the study subjects.

Results of laboratory tests and colonoscopic findings, including histologies for polyp, were extracted from clinical reports. Written informed consent was obtained from study participants. The study protocol has been approved by the ethics committee of Kyushu University.

Study subjects

The present study used data from April 1999 through March 2002. Among 2,390 male Self-Defense Forces officials who underwent the examination, 2,370 (99 percent) agreed to participate in the present study. After excluding men with histories of cancer, stroke, myocardial infarction, coronary revascularization, inflammatory bowel diseases, colorectal surgery, or diabetes mellitus, we kept 2,141 men in the analysis of dietary patterns. Of these, we excluded men who did not receive colonoscopy ($n = 57$), who underwent partial or unsuccessful colonoscopy ($n = 177$), or who had colorectal polyp removal prior to the examination ($n = 148$). Of the remaining 1,759 subjects who completed total colonoscopy, 764 men were identified as having colorectal polyps including hyperplastic nodules. Of these, 476 men had their polyps histologically confirmed: cancer ($n = 1$), carcinoid ($n = 1$), adenoma ($n = 346$), and other histologies ($n = 128$). Only 29 men had adenomas of 10 mm or larger, and nine had tubulovillous or villous adenomas. The data for the 346 men who had adenoma (case group) and 995 men who were free from any colorectal polyp and cancer (referent group) were analyzed to assess the association between dietary patterns and colorectal adenomas.

Dietary assessment

Information about diet was collected using a food frequency questionnaire designed to assess the average intakes of 74 food items, food groups, and food preparations over the previous year. The questionnaire was an expanded version of a 45-item food frequency questionnaire that was developed on the basis of a published questionnaire (24) and was validated against the 28-day dietary record (25). The expansion of food items was done with reference to food consumption in the National Nutrition Survey (19) and a dietary questionnaire developed elsewhere in Japan (26). Participants were asked to choose from seven response options for most dietary items, ranging from "never/less than one per month" to "two to three times per day." Different response schemes were used for green tea, coffee, and rice (five options) and for alcoholic beverages (six options). Daily consumers of green tea, coffee, or rice were asked about the number of cups or bowls consumed per day. Current drinkers, defined as those who have consumed alcoholic beverages weekly for at least 1 year in their lifetime and who were drinking at the time of the survey, were asked about the frequency of consumption and the amount of consumption per occasion of five alcoholic beverages, that is, sake (a Japanese wine), shochu (a Japanese distilled beverage), beer, whiskey, and wine. The amount of consumption per occasion was used in the estimation of total ethanol intake from these alcoholic beverages, but only the frequency of consumption for each alcoholic beverage was used in the analysis of dietary patterns.

Grouping of food factors

Before the analysis of dietary patterns, intakes of green tea, coffee, or rice were converted into units of cups or bowls per day, while those of other dietary items were quantified in terms of frequency per week. Five dietary questions that overlapped with or were duplicated by others (collective consumption of cooked vegetables, apples, mandarin oranges, other oranges, watermelons) and three questions about food spreads (butter, margarine, and jam/honey) were not used. Furthermore, some foods or food groups similar in nutritional content or culinary use were combined, leaving 39 food items for the purposes of the present study.

Statistical analysis

Dietary patterns were generated by factor analysis (principal components) using SAS PROC FACTOR statistical software (27). Factor analysis is a technique to reduce a number of variables into fewer independent factors. To make interpretation easier, a linear transformation called a "rotation" is normally performed on the initial factor solution. We used an orthogonal rotation procedure (varimax rotation), which maintains the uncorrelated nature of the factors and tries to get the original variables to load high on one of the factors and low on the rest. When factor scores are used as

independent variables in a subsequent regression analysis, this procedure has the advantage over oblique rotation that the analysis is less subject to problems of collinearity. In determining the number of factors to retain, we consider eigenvalue, the scree test, and interpretability. Eleven factors satisfied the criteria for eigenvalues greater than one, and the scree plot showed small breaks in the eigenvalues after factor 5, suggesting three or four factors to retain. Post-rotated factor loadings revealed that three factors well describe distinctive dietary patterns of the study population.

We thus retained the three dietary patterns and designated them as 1) a high-dairy, high-fruit and -vegetable, high-starch, low-alcohol (DFSA) pattern; 2) an "animal food" pattern; and 3) a Japanese pattern, according to the food items showing high loading (absolute value) with respect to each dietary pattern. We confirmed that these three dietary factors emerged when all 74 food items in our questionnaire were simply included in factor analysis. A factor score for each dietary pattern was calculated by weighting consumption of each food item by the corresponding factor loading and summing the resulting values. This score ranks individuals in terms of how closely they conform to the dietary pattern.

The potential confounding variables considered were hospital (Fukuoka or Kumamoto), age (treated as a continuous variable), parental history of colorectal cancer (absent or present), occupational rank (three categories), body mass index (<22, 22–23.9, 24–25.9, and ≥26 kg/m^2), smoking (lifetime nonsmoker, former smoker, and current smoker using <15, 15–24, or ≥25 cigarettes/day), and leisure-time physical activity, expressed as the sum of metabolic equivalents for each activity multiplied by the corresponding hours of such activity per week (none, <20, 20–39.9, and ≥40 metabolic equivalent-hours). Quartiles of factor scores of each dietary pattern among controls were used for cutoff values. Multiple logistic regression that included terms for the above-mentioned variables was performed to estimate the odds ratio and 95 percent confidence interval of colorectal adenomas according to quartiles of scores for each dietary pattern, taking the lowest quartile group as the referent group. Analyses were repeated for adenomas of 5 mm or larger (n = 140) or according to the location of the lesion (proximal colon including the cecum, ascending colon, liver flexure, transverse colon, and splenic flexure; distal colon including the descending colon and sigmoid colon; and the rectum). Logistic regression analysis was performed using SAS PROC LOGISTIC software (27).

RESULTS

Table 1 shows factor loadings, which are equivalent to simple correlations between the food items and the dietary patterns. A positive loading indicates that the food item is positively associated with the dietary pattern, and a negative loading indicates an inverse association with the dietary pattern. The DFSA dietary pattern was characterized by frequent intake of fermented dairy products, milk, confectionaries, bread, fruits, and vegetables and infrequent intake of shochu, a local alcoholic beverage in the study areas. The "animal food" dietary pattern was characterized by various kinds of animal foods, including red meat, poultry, seafood excluding fish, processed meat and fish products, and fried or broiled foods. The Japanese dietary pattern was characterized by traditional foods in Japan (soybean products, seaweed, pickles, and green tea), vegetables, and fish. The proportion of the total variance explained by the three factors was 24 percent.

TABLE 1. Factor-loading matrix for dietary patterns, Self-Defense Forces Health Study, Japan, 1999–2002*

	DFSA† dietary pattern	"Animal food" dietary pattern	Japanese dietary pattern
Fermented dairy products	0.61	–	–
Confectionaries	0.55	0.18	–
Canned fruits	0.52	–	–
Bread	0.47	–	–0.39
Fruits (not canned)	0.47	–	0.21
Fruit juices	0.47	–	–
Vegetable juice	0.41	–	0.17
Milk	0.40	–	–
Oil dressing	0.33	0.19	0.26
Soda, cola	0.30	0.20	–0.18
Shochu (alcoholic beverage)	–0.40	0.15	0.24
Red meat	–	0.68	–
Poultry	–	0.63	–
Fried foods	0.25	0.49	0.29
Broiled fish/meat	–	0.48	0.32
Seafood (except fish)	–	0.47	0.18
Processed meat	0.17	0.46	–
Processed fish	–	0.41	0.18
Gyoza‡	–	0.40	–
Liver	–	0.38	–
Eggs	–	0.34	0.22
Noodles	–	0.34	–
Soybean products	–	–	0.64
Cooked vegetables	0.36	0.23	0.56
Seaweed	0.27	–	0.55
Raw vegetables	0.45	–	0.52
Pickles	0.19	–	0.51
Green tea	–	–0.15	0.46
Fish	–	0.27	0.38
Potatoes	0.33	0.24	0.35
Garlic	0.20	–	0.32
Variance explained (%)	8.5	7.9	7.7

* Factor loadings are equivalent to simple correlations between the food items and the dietary patterns. Factor loadings less than ±0.15 were indicated by a dash; food items with factor loadings less than ±0.30 for all dietary patterns (rice, mayonnaise, nuts, coffee, wine, beer, whiskey, sake) were omitted.

† DFSA, high-dairy, high-fruit and -vegetable, high-starch, low-alcohol (dietary pattern).

‡ Dumpling with minced pork and vegetable stuffing.

TABLE 2. Dietary patterns in relation to potential confounding variables and alcohol intake among referents, Self-Defense Forces Health Study, Japan, 1999–2002

Dietary patterns	Hospital (% Kumamoto)	Age (mean years)	Rank (% highest)	Parental history of colorectal cancer (%)	Body mass index (mean kg/m²)	Smoking (% current smokers)	Physical activity (median metabolic equivalent-hours)	Alcohol (median ml/day)*
DFSA† dietary pattern								
Quartile 1 (low)	28	52.4	10	6	23.7	45	15	62
Quartile 2, 3	27	52.4	14	4	24.0	38	16	32
Quartile 4 (high)	18	52.4	19	5	23.5	40	16	14
p_{trend}‡	0.01	0.49	<0.01	0.66	0.46	0.26	0.84	<0.01
"Animal food" dietary pattern								
Quartile 1 (low)	30	52.5	15	4	23.6	40	16	14.5
Quartile 2, 3	24	52.4	14	4	23.8	42	16	34
Quartile 4 (high)	22	52.3	13	6	23.9	37	15	49
p_{trend}	0.05	0.23	0.43	0.52	0.15	0.56	0.87	<0.01
Japanese dietary pattern								
Quartile 1 (low)	21	52.4	17	5	23.7	48	9.5	21
Quartile 2, 3	25	52.3	13	4	23.8	39	16	40
Quartile 4 (high)	29	52.5	14	4	23.9	36	19	38
p_{trend}	0.02	0.58	0.51	0.66	0.51	<0.01	<0.01	<0.01

* Estimated from the consumption of five alcoholic beverages: beer, sake, shochu, wine, and whiskey.
† DFSA, high-dairy, high-fruit and -vegetable, high-starch, low-alcohol (dietary pattern).
‡ Mantel-Haenszel chi-squared test for categorical variables and linear regression analysis for continuous variables, assigning to categories of each dietary pattern their median scores (physical activity and alcohol consumption were log transformed).

Table 2 shows the association of dietary patterns with potential confounding variables and alcohol consumption among men free from colorectal polyp or cancer (referent group). Examinees at the Kumamoto hospital had a higher score for the Japanese dietary pattern but lower scores for the DFSA and "animal food" dietary patterns than those at the Fukuoka hospital. This reflects the geographic characteristics of dietary patterns; the southern parts of Kyushu Island, including Kumamoto, are less urbanized than the northern parts, including Fukuoka. Men with a high score for the DFSA dietary pattern tended to have higher occupational positions and consumed smaller amounts of alcohol. Men with high scores for the "animal food" dietary pattern tended to consume greater amounts of alcohol. Men in the upper quartiles of the Japanese dietary pattern tended to be nonsmokers and engaged in higher levels of leisure-time physical activity, and they consumed greater amounts of alcohol.

As shown in table 3, the DFSA dietary pattern was inversely associated with the risk of colorectal adenomas, showing a 40 percent reduced odds ratio among men in the highest quartile of the dietary pattern compared with those in the lowest. This association was slightly more evident for adenomas with a diameter of 5 mm or larger. No apparent association was observed for either the "animal food" dietary pattern or the Japanese dietary pattern.

The DFSA dietary pattern was inversely associated with adenomas at all subsites of the colorectum (table 4). The association was slightly stronger for the proximal colon in terms of the odds ratio of 0.5 for the highest quartile of the dietary pattern score and test for the trend association ($p_{trend} = 0.003$), but the confidence intervals of odds ratios for this site overlapped substantially with those for other sites. The Japanese and "animal food" dietary patterns were not measurably associated with colon adenomas. However, a nonsignificant positive association with rectal adenomas was observed for the Japanese pattern, while a nonsignificant inverse association was found for the "animal food" pattern. The odds ratios for the upper three quartiles combined compared with the lowest were 1.64 (95 percent confidence interval: 0.83, 3.25) and 0.64 (95 percent confidence interval: 0.36, 1.13) for the Japanese pattern and "animal food" pattern, respectively.

DISCUSSION

We investigated the association between major dietary patterns and colorectal adenomas among middle-aged Japanese men. Of the three dietary patterns we identified, the DFSA dietary pattern showed a significant, inverse association with the risk of colorectal adenomas.

Strengths and limitations

Our study had several strengths. Selection bias in terms of study participation was unlikely because of nonselective

TABLE 3. Logistic regression results for the association between dietary patterns and colorectal adenoma, Self-Defense Forces Health Study, Japan, 1999–2002

Dietary pattern	Quartile*							p_{trend}
	1 (low)	2		3		4 (high)		
		Odds ratio†	95% confidence interval	Odds ratio	95% confidence interval	Odds ratio	95% confidence interval	
DFSA‡ dietary pattern								
Adenoma of any size	1.00	0.97	0.70, 1.36	0.71	0.50, 1.01	0.62	0.43, 0.90	0.003
Adenoma of 5 mm or larger	1.00	0.84	0.52, 1.34	0.68	0.41, 1.12	0.59	0.35, 0.996	0.04
"Animal food" dietary pattern								
Adenoma of any size	1.00	0.87	0.61, 1.23	0.91	0.64, 1.28	0.86	0.60, 1.23	0.49
Adenoma of 5 mm or larger	1.00	1.05	0.64, 1.72	0.84	0.50, 1.41	0.98	0.59, 1.63	0.75
Japanese dietary pattern								
Adenoma of any size	1.00	0.96	0.67, 1.38	1.13	0.79, 1.61	1.18	0.83, 1.69	0.26
Adenoma of 5 mm or larger	1.00	1.00	0.59, 1.70	1.11	0.66, 1.86	1.24	0.75, 2.08	0.36

* Among referents.
† Adjusted for hospital, age, parental history of colorectal cancer, occupational rank, body mass index, smoking, and leisure-time physical activity.
‡ DFSA, high-dairy, high-fruit and -vegetable, high-starch, low-alcohol (dietary pattern).

recruitment for the preretirement health examination, which included total colonoscopy as a routine procedure, and high study participation rate. The questionnaire was distributed and collected prior to colonoscopy, and thus recall bias associated with adenoma status was also unlikely. The control series consisted of only subjects who were confirmed via total colonoscopy to be free from any colorectal polyp and cancer, leading to a more valid assessment compared with studies

TABLE 4. Logistic regression results for the association between dietary patterns and colorectal adenoma according to the location of the lesion, Self-Defense Forces Health Study, Japan, 1999–2002

Dietary pattern	Quartile*							p_{trend}
	1 (low)	2		3		4 (high)		
		Odds ratio†	95% confidence interval	Odds ratio	95% confidence interval	Odds ratio	95% confidence interval	
Colon adenoma (n = 299)								
DFSA‡ dietary pattern	1.00	0.93	0.66, 1.32	0.70	0.48, 1.01	0.59	0.40, 0.87	0.003
"Animal food" dietary pattern	1.00	0.93	0.64, 1.35	0.97	0.67, 1.40	0.95	0.65, 1.38	0.85
Japanese dietary pattern	1.00	0.93	0.64, 1.37	1.09	0.76, 1.59	1.11	0.77, 1.62	0.45
Proximal colon adenoma (n = 158)								
DFSA dietary pattern	1.00	1.00	0.64, 1.54	0.67	0.41, 1.09	0.50	0.30, 0.85	0.003
"Animal food" dietary pattern	1.00	0.84	0.51, 1.39	1.08	0.68, 1.73	0.94	0.57, 1.53	0.95
Japanese dietary pattern	1.00	0.87	0.53, 1.42	0.92	0.56, 1.49	1.08	0.67, 1.74	0.70
Distal colon adenoma (n = 171)								
DFSA dietary pattern	1.00	1.00	0.64, 1.54	0.77	0.48, 1.23	0.68	0.42, 1.11	0.08
"Animal food" dietary pattern	1.00	1.01	0.63, 1.62	0.95	0.59, 1.52	1.01	0.63, 1.62	0.97
Japanese dietary pattern	1.00	1.10	0.67, 1.79	1.43	0.90, 2.28	1.21	0.74, 1.96	0.35
Rectal adenoma (n = 63)								
DFSA dietary pattern	1.00	0.94	0.48, 1.84	0.64	0.30, 1.36	0.71	0.34, 1.48	0.26
"Animal food" dietary pattern	1.00	0.66	0.33, 1.34	0.64	0.31, 1.32	0.62	0.30, 1.28	0.22
Japanese dietary pattern	1.00	1.58	0.71, 3.51	1.56	0.70, 3.47	1.79	0.82, 3.92	0.18

* Among referents.
† Adjusted for hospital, age, parental history of colorectal cancer, occupational rank, body mass index, smoking, and leisure-time physical activity.
‡ DFSA, high-dairy, high-fruit and -vegetable, high-starch, low-alcohol (dietary pattern).

based on partial colonoscopy. We controlled for major known or suspected confounding factors. The uniform background of the study subjects in terms of occupation, sex, and age was also advantageous in maintaining comparability between cases and controls, although this uniformity limits the extent to which we may generalize from the present findings.

The present study also features some limitations. For one, the dietary questionnaire has not been validated. However, the former version, including questions and response options similar to those of the present questionnaire, has been validated against 7-day, year-round dietary records (25). Most nutrients and foods demonstrated fairly good correlation between the dietary record and questionnaire; relatively high correlation coefficients of 0.80, 0.77, 0.58, and 0.58 were observed for bread, fruits, dairy products, and pickled vegetables, respectively. Nondifferential misclassification in our dietary assessment could distort risk estimates toward the null. Such a bias may be minimal for the analysis of the DFSA dietary pattern, composed of food items showing good correlation between the dietary record and questionnaire, but this bias could be the reason for the lack of an apparent association with the "animal food" or Japanese dietary pattern.

Limitations of factor analysis arise from the arbitrary decisions (15) involved in selecting and grouping foods for analysis from the questionnaire, in determining the number of factors to retain, in choosing the method of rotation of the initial factors to increase the interpretability of the dietary pattern, and in labeling dietary patterns according to their factor loadings. Masaki et al. (28) identified four major dietary patterns using baseline data of a cohort of male employees in Tokyo. Similar to our study, their study identified a "Western breakfast" dietary pattern and an "animal" dietary pattern, suggesting the existence of dietary patterns common to the Japanese. Our derived dietary patterns accounted for 24 percent of the total variance, which is comparable with a figure observed in a previous study (17) but less than that reported in a Japanese study (28). Caution needs to be exercised when comparing the variance explained across studies, which is determined by various factors including the number of variables in analysis.

Interpretation of findings

A dietary pattern characterized by frequent intakes of dairy products, confectionaries, and fruits and vegetables, as well as by infrequent consumption of shochu, a local alcoholic beverage, was inversely associated with the risk of colorectal adenomas. This dietary pattern seems to consist of relatively healthy selections of foods found in Western countries and includes foods of probably low consumption in Japan. According to the food balance sheet (29), per capita supplies of dairy products in Japan and among developed countries in the year 2001 were 66 kg (181 g/day) and 197 kg (540 g/day), respectively; the corresponding values for fruits were 53 kg (145 g/day) and 83 kg (227 g/day). Although the associations between these foods and colorectal cancer have been inconsistent, the present results are in agreement with the existing body of evidence, including findings from recent studies, indicating that high consumption of dairy products or calcium (30–34) and high consumption of fruits, fruit juices, or fruit fiber (10, 35–38) are each associated with reduced risk of colorectal cancer or adenoma. A positive association of alcohol consumption and colorectal adenomas or cancer has been reported in many studies, including those in Japan (23, 39). In addition to independent effects, there may be complex interactions among food factors constituting the DFSA dietary pattern. For example, fruit juices may enhance calcium absorption (40), and reduced alcohol intake increases the bioavailability of folate (41). The glycemic effects of a high-starch or a high-sugar diet and their contribution to increased risk of colorectal cancer have been suspected, but epidemiologic findings are inconsistent on this point (42, 43). Our finding of an inverse association between the DFSA dietary pattern and colorectal adenomas provides the following suggestions: that a high-starch diet may inhibit, rather than promote, the formation of colorectal adenomas and that the adverse effects of a high-starch diet, if any, may not be so strong as to negate the protective effects of other foods contributing to this dietary pattern on adenoma risk. The inverse association of this dietary pattern with adenoma risk was somewhat stronger for the proximal colon than for other sites. Random error could be an explanation. Alternatively, the dietary pattern may be more closely involved in the formation of adenomas in the proximal colon.

The Japanese dietary pattern was characterized by high consumption of many plant foods, including traditional Japanese foods (soybean products, seaweed, pickles) and vegetables. A diet rich in various plant foods could potentially reduce cancer risk because of their many biologically active chemicals (44). However, the Japanese dietary pattern was not apparently associated with colonic adenomas. In studies of Western populations, inverse associations between similar dietary patterns (designated "prudent" or "healthy" patterns) and colorectal cancer have been unclear (18) or limited to subgroups (17). The lack of such an association in our study may contradict a body of evidence supporting an inverse association between vegetables and colorectal cancer (4) but agree with results of recent prospective, but not all (10, 37), studies reporting no association between vegetables or fiber and colorectal cancer or adenoma (5–8). As most of the adenomas in the present study were small in size and less malignant in nature, the present finding is in line with a hypothesis that vegetables are inversely associated with the progression of colorectal adenomas to cancer but not with the initial appearance of adenomas (38). We found a nonsignificant positive association between the Japanese dietary pattern and the risk of rectal adenomas. Studies in Japan (45–49) have consistently shown that frequent consumption of preserved foods including pickled vegetables and dried/salted fish, typical of the Japanese diet, is associated with increased risk of colorectal cancer; of these studies, three documented a significant association specifically for the rectum (46–48). These preserved foods contain *N*-nitroso compounds (50), which are potent carcinogens (51). Among other foods characterizing the Japanese pattern, broiled fish is a potential source of exposure to carcinogenic heterocyclic amine (52), although we are not aware of any epidemiologic

findings suggesting a relation between broiled fish and colorectal cancer risk.

Meat, especially red meat, processed meat, or meat broiled at high temperature, has been associated with colorectal cancer (53, 54) or adenoma (55). A study in Japan found a significant positive association between intake of animal protein and the risk of colorectal adenoma (56). However, we find no increase in the risk of colorectal adenomas associated with the "animal food" dietary pattern. Besides possible bias due to misclassification in the dietary assessment (as discussed above), the lack of such an association for colon adenomas in our study may be attributable to the moderate consumption of meat in Japan (mean daily intake of total meat: 96 g for men aged 40–49 years (19)). In addition, poultry has contributed to the healthy or prudent dietary patterns in Western populations (16–18). The diversity of animal food sources may dilute the potential carcinogenic effects of a specific animal food. Furthermore, it is possible that moderate intake of animal foods prevents carcinogenesis because these foods provide nutrients such as methionine and folate, which are beneficial in DNA synthesis and DNA methylation (57). In this context, our finding showing an increased risk of rectal adenomas associated with the lowest quartile of the "animal food" pattern may be of note and is consistent with results of certain studies relating to colorectal cancer in Japan (45, 48, 58).

In conclusion, the present results indicate that a dietary pattern characterized by frequent consumption of dairy products, confectionaries, bread, fruits, and vegetables but low intake of local alcoholic beverages is associated with a reduced risk of colorectal adenomas in Japanese men. Nonsignificant associations for rectal adenomas, based on an analysis including only 63 men with adenomas in the rectum, should set a limit to causal inference. However, since the incidence of rectal cancer in Japan has been high among industrial countries (12), the question as to whether a Japanese-style diet or a diet low in animal foods promotes carcinogenesis of the rectum warrants further investigation.

ACKNOWLEDGMENTS

This work was supported by a grant-in-aid for scientific research on priority areas (12218226) from the Ministry of Education, Culture, Sports, Science, and Technology, Japan, and by a Health and Labor Sciences research grant for research on cancer prevention and health services research from the Ministry of Health, Labor, and Welfare, Japan.

The authors thank the ward nurses of Self-Defense Forces Fukuoka and Kumamoto hospitals for their assistance in conducting the study.

REFERENCES

1. Buell P, Dunn JE. Cancer mortality among Japanese Issei and Nisei of California. Cancer 1965;18:656–64.
2. Tominaga S. Cancer incidence in Japanese in Japan, Hawaii, and western United States. Natl Cancer Inst Monogr 1985;69: 83–92.
3. Shimizu H, Mack TM, Ross RK, et al. Cancer of the gastrointestinal tract among Japanese and white immigrants in Los Angeles County. J Natl Cancer Inst 1987;78:223–8.
4. Glade MJ. Food, nutrition, and the prevention of cancer: a global perspective. American Institute for Cancer Research/World Cancer Research Fund, American Institute for Cancer Research. Nutrition 1999;15:523–6.
5. Michels KB, Giovannucci E, Joshipura KJ, et al. Prospective study of fruit and vegetable consumption and incidence of colon and rectal cancers. J Natl Cancer Inst 2000;92:1740–52.
6. Fuchs CS, Giovannucci EL, Colditz GA, et al. Dietary fiber and the risk of colorectal cancer and adenoma in women. N Engl J Med 1999;340:169–76.
7. Schatzkin A, Lanza E, Corle D, et al. Lack of effect of a low-fat, high-fiber diet on the recurrence of colorectal adenomas. Polyp Prevention Trial Study Group. N Engl J Med 2000;342:1149–55.
8. Alberts DS, Martinez ME, Roe DJ, et al. Lack of effect of a high-fiber cereal supplement on the recurrence of colorectal adenomas. Phoenix Colon Cancer Prevention Physicians' Network. N Engl J Med 2000;342:1156–62.
9. Bingham SA, Day NE, Luben R, et al. Dietary fibre in food and protection against colorectal cancer in the European Prospective Investigation into Cancer and Nutrition (EPIC): an observational study. Lancet 2003;361:1496–501.
10. Peters U, Sinha R, Chatterjee N, et al. Dietary fibre and colorectal adenoma in a colorectal cancer early detection programme. Lancet 2003;361:1491–5.
11. Statistics and Information Department, Minister's Secretariat, Ministry of Health, Labor, and Welfare. Age-adjusted death rates by prefecture. In: Special report on vital statistics, 2000. (In Japanese). Tokyo, Japan: Japan Health and Welfare Statistics Association, 2002.
12. Parkin DM, Whelan SL, Ferlay J, et al, eds. Cancer incidence in five continents. Vol VIII. Lyon, France: International Agency for Research on Cancer, 2002. (IARC publication no. 155).
13. Honda T, Kai I, Ohi G. Fat and dietary fiber intake and colon cancer mortality: a chronological comparison between Japan and the United States. Nutr Cancer 1999;33:95–9.
14. Kono S, Ahn YO. Vegetables, cereals and colon cancer mortality: long-term trend in Japan. Eur J Cancer Prev 2000;9:363–5.
15. Jacques PF, Tucker KL. Are dietary patterns useful for understanding the role of diet in chronic disease? Am J Clin Nutr 2001;73:1–2.
16. Slattery ML, Boucher KM, Caan BJ, et al. Eating patterns and risk of colon cancer. Am J Epidemiol 1998;148:4–16.
17. Terry P, Hu FB, Hansen H, et al. Prospective study of major dietary patterns and colorectal cancer risk in women. Am J Epidemiol 2001;154:1143–9.
18. Fung T, Hu FB, Fuchs C, et al. Major dietary patterns and the risk of colorectal cancer in women. Arch Intern Med 2003;163: 309–14.
19. Bureau of Public Health, Ministry of Health and Welfare. The national nutrition survey in Japan, 1996. (In Japanese). Tokyo, Japan: Daiichi Shuppan, 1998.
20. Hill MJ, Morson BC, Bussey HJ. Aetiology of adenoma-carcinoma sequence in large bowel. Lancet 1978;1:245–7.
21. Vogelstein B, Fearon ER, Hamilton SR, et al. Genetic alterations during colorectal-tumor development. N Engl J Med 1988;319:525–32.
22. Kono S, Handa K, Hayabuchi H, et al. Obesity, weight gain and risk of colon adenomas in Japanese men. Jpn J Cancer Res 1999;90:805–11.
23. Toyomura K, Yamaguchi K, Kawamoto H, et al. Relation of cigarette smoking and alcohol use to colorectal adenomas by